April 2010

The Effects of Material and Configuration on the Acoustic Response of an Impact Stop

Adam Barnes Belanger
Worcester Polytechnic Institute

Daniel Richard Mallette
Worcester Polytechnic Institute

John Richard Meade
Worcester Polytechnic Institute

The Effects of Material and Configuration on the Acoustic Response of an Impact Stop

A Major Qualifying Project

Submitted to the Faculty

Of the

WORCESTER POLYTECHNIC INSTITUTE

In Partial Fulfillment of the Requirements for the

Degree of Bachelor of Science

By

_____

Adam B. Belanger

_____

Daniel R. Mallette

_____

John R. Meade

_____

Professor Diana A. Lados

_____

Professor Robert L. Norton

ACKNOWLEDGEMENTS

This project would not have been possible without the aid of a number of members of the WPI community. The team would like to acknowledge the following individuals in particular for their time and effort:

- Professor Diana A. Lados
- Professor Robert L. Norton
- Corey Maynard
- Anastasios Gavras
- Doug Peterson
- Dr. Boquan Li
- Adam Sears
- Torbjorn Bergstrom

ABSTRACT

The noise levels on factory floors have been historically a concern with respect to workers' health. The goal of this project was to investigate various materials and configurations that will minimize noise output upon repetitive impact. This was accomplished by first constructing a sound testing and evaluation system, then preparing testing prototypes and evaluating their sound responses, and ultimately optimizing the materials and geometries for acoustic dampening. These results could be beneficially implemented for various applications including impact stops in production facilities where each stop is hit hundreds of times per minute contributing to high decibel levels on the production floor – i.e., applications which require both strength for dimensional accuracy and low acoustic response. The results and findings from this investigation will be presented and discussed.

EXECUTIVE SUMMARY

Permanent hearing loss due to sound levels in the workplace has been a historical cause for concern. Every year over 300,000 healthy life years are lost due to occupational hearing loss in developed countries, nearly 4 million in developing countries (1). Our sponsor recognizes this issue and has begun the process of reducing noise levels on their production floors. Methods such as encasing a machine inside a sound proof box have proven effective but expensive. As such, a cheaper and easier method of sound reduction is desired. One identified source of high sound levels are impact stops which are utilized on many of the production machines. An impact stop is a small piece of hardened tool steel which is ground to a specific height in order to control the stopping location of an arm driven by a cam.

One of the goals of this project was to identify changes in material and configuration of the impact stop which result in the greatest decrease in sound output. Additionally, changes in the material of the hammer which impacts the stop were examined. A second goal for this project was to develop a testing procedure that produced consistent, repeatable, and reliable results.

In order to achieve these results a detailed methodology was developed. One of the first steps was proper material selection. Our research indicated that two material properties relevant to this project were Mechanical Loss Coefficient (a materials ability to dissipate vibration) and Young's Modulus (the stiffness of a material). Using Granta software, a variety of different metals was selected. Additionally, the affect of porosity on sound was a topic of interest, so two types of porous metals were obtained. A thorough microstructural analysis was done on all of

the materials in an attempt to fine correlation between microstructure and the sound output during testing.

Material prototypes for the impact stops were developed in several configurations:

- Single Material Stop
  - The same geometry with only variable being material from prototype to prototype
- Cored Stop
  - Had a hole drilled in the center of the stop and filled with a damping material
- Coated Stop
  - Had a polymer coating around the circumference of the stop
- Cored and Coated
  - Had a hole drilled in the stop and filled with a polymer, in addition to a polymer coating around the circumference of the stop.

A testing apparatus was developed using as much of the sponsors original machinery as possible, this was done to as closely as possibly replicate the end conditions on the actual production machines. A solenoid driven ram was connected to the slide and the slide housing was secured to a base plate.

After running the prototype stops and hammers on the testing apparatus, some clear results were obtained. All stops with a changed configuration (cored, coated, etc.) performed better than a single material stop. Changing the material of the hammer further reduced the sound output upon impact, leading to a maximum tested sound reduction of 2.4 dBA. Observations between microstructure and sound output were seen. However, a more in depth study is required before any conclusive statements can be made in that area. Additionally, a relationship between the ratio of a material's Young's Modulus / Hardness to the sound output was seen; however, more data are needed in this case to further validate the relationship.

TABLE OF CONTENTS

TABLE OF FIGURES

TABLE OF TABLES

1 INTRODUCTION

Workplace conditions play a major role in the efficiency of a business. Companies in the manufacturing sector typically have employees working close to machines, and therefore, a safe workplace environment is essential. This includes safety not only from immediate physical dangers, but also, from long-term dangers, such as degradation of hearing due to excessive sound levels. Studies have shown that extensive exposure to sound levels equal to or higher than 85 decibels can cause the loss of hearing. In many manufacturing settings, such as those of the sponsor, sound levels emitted by machines on the assembly line have frequently been recorded at higher levels than 85 decibels. In these conditions, hearing protection must be worn. Other than the cost of providing hearing protection, its use is also an inconvenience to those on the floor, often hindering important communication, or not providing sufficient protection

One particular component of assembly line machines that has been identified as a source of increased sound levels is a hard stop. A hard stop consists of a piece of hardened tool steel mounted at a fixed location to provide a controlled stop while maintaining tolerance of location. A slider mechanism of hardened tool steel repeatedly drives up against the hard stop, creating a loud noise. The slider must strike the hard stop in the same location every time to ensure accuracy; therefore the hard stop must remain dimensionally stable. The hard stop is in the shape of a "T" and is shown in Figure 1.

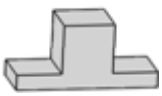

FIGURE 1: ORIGINAL HARD STOP GEOMETRY.

AISI A6 tool steel was selected for the hard stop material most likely due to its inherent strength, durability, and hardness. Although the hard stops are engineered well for strength, they exhibit poor acoustic damping properties.

The sponsor has already started to take measures to reduce the sound levels on assembly line machines. Many new machines have redesigned cams which reduce velocity at the point where impact occurs. This reduced the force impacting the stop, and reduced some of the noise produced. Some machines have also been enclosed in sound dampening units. These units encase the machine entirely with several access doors for maintenance and, it should go without saying, these enclosures are expensive and make access to the machine more difficult.

Reducing noise through a redesign of the hard stops will be cheaper than other noise damping mechanisms (such as enclosing units) and can be easily retrofitted to current machines. Therefore, the goal of this project is to reduce the audible noise output of the hard stop impact, while maintaining accuracy in the production process. This is accomplished through a combined method by concomitantly re-evaluating the material used and redesigning the geometry of the hard stop and the hammer that impacts the hard stop.

2 BACKGROUND

This section discusses topics that were researched to evaluate their possible role in reducing noise emissions from a mechanical stop. Research into currently implemented noise reduction techniques was conducted to have a working knowledge of why certain materials or designs are good candidates for noise reduction. Topics such as diffusion bonding and brazing were researched in order to understand ways to effectively connect materials, specifically, layering different materials. Not much is known about the effects of cryogenic freezing on materials acoustic properties, however, it was researched to help determine if there is an effect on acoustics or acoustical dampening.

2.1 Sound Absorbers

There are three main categories of sound absorbing materials: porous materials, panel absorbers, and resonators (2). The mounting of the absorber has a large bearing on the effectiveness. Each one acts through a different mechanism of sound absorption or dampening. Below are brief descriptions of each method.

Porous materials - These materials contain voids that convert acoustic energy to heat, dissipating the sound that goes through them. Thickness of the coating plays an important part in how effective the sound dampening is. Thicker configurations of porous materials increase low frequency absorption (3).

Panel Absorbers - These structures have membranes that respond to sound pressure exerted by adjacent air molecules by flexing. Panels are most efficient at absorbing low frequencies. Due to the requirements of the project, this technique is not likely to be utilized.

Resonators - These are structures with holes or slots connected to a trapped quantity of air. Resonators act on a narrow band of frequency. What frequency is absorbed depends on the shape of the cavity. The resonant frequency is governed by the size of the opening, the length of the neck, and the volume of air trapped in the chamber. Typically, perforated materials only absorb the mid-frequency range. Due to the part geometries for this project, this technique will most likely not be utilized.

Based on our research, porous materials appear to be the best candidate for a sound absorption coating to be incorporated in the sponsor's impact stop. Several types of porous materials were looked into, such as polyurethane based foams, fiber glass, activated carbon fiber, and spray cellulose.

It is well documented that polyurethane foams are useful in absorbing sound due to their porous structure. It can come as an open or closed cell structure and can be sprayed on. Open cell foams are considered better for sound absorption, but are soft and not recommended for uses that require strength or rigidity (4). Figure 2 shows the effect of thickness on frequency absorption by closed cell polyurethane spray foams (5).

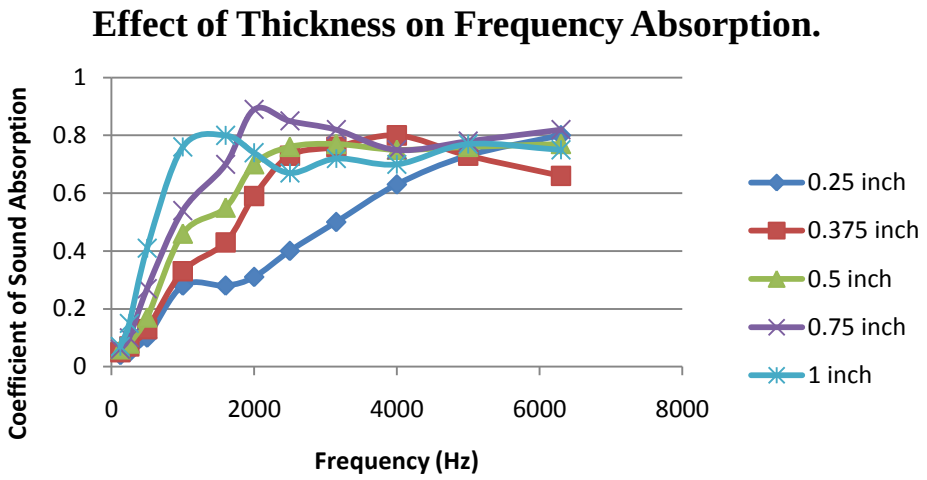

FIGURE 2: EFFECT OF THICKNESS OF POLYURETHANE SPRAY FOAM SOUND ABSORPTION ON PARTICULAR FREQUENCIES

Fiberglass can be used for sound absorption, but research has shown it has been more commonly used for thermal and sound insulation in residential settings rather than industry. Sprayed cellulose is claimed to insulate sound better than fiberglass. Carbon fiber is used in automotive fields for both high strength to weight ratio and sound absorbing properties. Activated carbon fibers are also being considered for sound dampening applications. This would be produced by adding carbon to a nonwoven fabric like cotton, then having it undergo cabonization and activation. Carbonization is a thermochemical process (pyrolysis), which converts carbonaceous materials into active carbon products. Activated carbon fiber nonwoven (ACF) has been shown to absorb higher incident sound waves than glass fibers or the nonwoven fabric alone.

Although there has been extensive research into sound absorbing materials, many fail to discuss the absorption of frequencies above 6000 Hz. Due to human hearing being in the range

of 20 – 20,000 Hz, and the peak sensitivity being at 4,000 Hz, the range of frequencies that need to be considered in the selection of sound absorbing materials had to be increased.

2.2 A-weighting

Sound affects human hearing in ways that differ from the sound pressure wave intensity. Human hearing is more sensitive to frequencies in the range of human speech, around 4000 Hz. To account for this phenomenon, a weighting scale is necessary to adjust the sound intensity at a given frequency to what human hearing would actually perceive.

Historically, A-weighting is the most common weighting form. More recent studies have shown that A-weighting may not be the most accurate way to consider perceived loudness, but A-weighting is still the only legally required weighting for sound measuring, so by using it readings could be easily compared with previous measurements. A-weighting may be inaccurate due to its original development and use for pure tones, and not for random noise. One concern about using A-weighting is that unless there is a filter to remove frequencies over 20 kHz, which aren't detectable by the human ear, the resulting readings will not be accurate. Another limitation of A-weighting is that it devalues low frequencies and therefore should not be used for less intense sound levels that have significant contributions from low frequencies (6). C-weighting is considered a better measurement for more impure tones with harmonics. B-weighting is a compromise between A and C weighting, and is generally considered to be less accurate.

The formula for A-weighting is shown in Equation 1.

$$R_A(f) = \frac{12200^2 * f^4}{(f^2+20.6^2)*(f^2+12200^2)*\sqrt{(f^2+107.7^2)*(f^2+737.9^2)}} \quad (1)$$

This equation takes the frequency analyzed and weighs it to reduce effects of frequencies under 1000 Hz and over 7000 Hz, while increasing the effects of the frequencies between these values. A method for converting this weighted value into a sound level in decibels is shown in Equation 2. Due to the weighting method, the value must be normalized, typically at 1000 Hz. This is the reason for addition of a value of 2 to the result.

$$dB = 2 + 20 * \log[R_A(f)] \quad (2)$$

The formula for C-weighting is shown in Equation 3.

$$R_C(f) = \frac{12200^2 * f^2}{(f^2+20.6^2)*(f^2+12200^2)} \quad (3)$$

The formula to converting C-weighted data into decibels is shown in Equation 4.

$$dB = 0.06 + 20 * \log[R_C(f)] \quad (4)$$

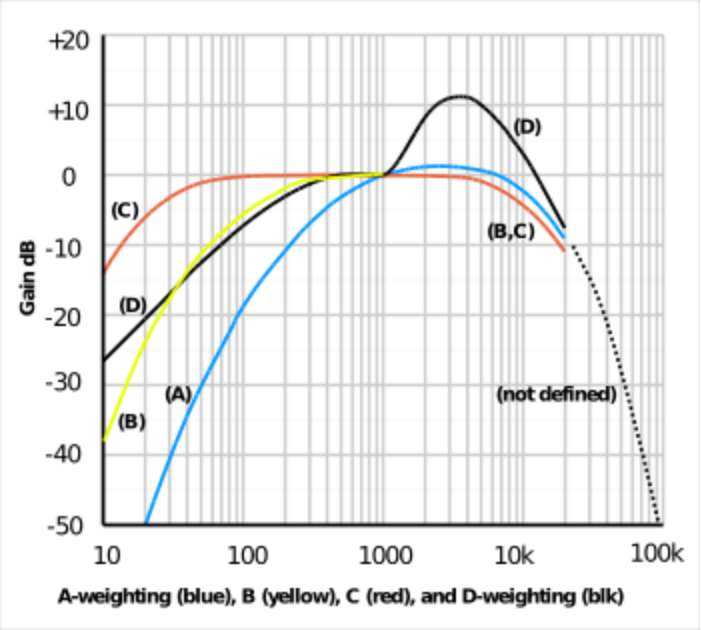

FIGURE 3 - SOUND LEVEL WEIGHTINGS.

For comparison purposes, a value that represents the "loudness" of the material must be calculated. Thus, taking the RMS average of the results, as shown in Equation 5, will yield a value of intensity that better reflects the perceived loudness. This will be used in this project.

$$RMS = \sqrt{\frac{x_1^2 + x_2^2 + x_3^2 \ldots x_n^2}{n}} \tag{5}$$

2.3 Sound Absorbing Materials

Materials that can withstand the required loads while also having sound absorbing qualities were investigated. Materials with controlled porosity represent an important class of materials for sound absorption. These materials retain many of the properties of their solid/fully dense counterparts, plus increased specific stiffness, sound absorbing capabilities, and low

thermal conductivities. There are several methods of creating a porous metal, and a few will be discussed here.

One method of producing a porous metal structure is by sintering metal fibers. This achieved by using a drawing method to make metal fibers in the size range of 50 – 100 μm in diameter (7). These fibers are pressed together to make a solid compact with controlled porosity. As porosity increases, higher frequencies are absorbed easier. Increasing fiber diameter shifts frequencies absorbed lower. Better sound performance is achieved by making a composite structure where the outer layer more porous than the inner layer (8) . If the outer layer is not very porous, it is the limiting factor on the sound absorbing capabilities, even if the subsequent layers are more porous. Layering differing materials with different porosity improves low frequency absorption, and helps higher frequency sound absorption as well.

Another technique that can be used to create porous metal is with the use of a foaming agent to create bubbles within a powder metallurgy part during firing (9). This is created by mixing metal powder and foaming agent compacting to form a dense semi-finished product without any residual open porosity. Porosity in the range of 40% - 90% can be achieved this way. Less than 1% of the foaming agent is required if metal hydrides are used typically.

A method of producing open celled porous metals is by using a polyurethane sponge as a template for a replication process. The template of reticulated polyurethane is then covered in a slurry infiltration. Then the template is thermally removed. The product is now debindered and referred to as a brown structure. This brown compact is then sintered. This method allows for cell size of 0.4 – 5.0 mm and porosity levels of 75 - 90%.

Another structure that uses a template is the hollow sphere structure. These are produced by a powder coating of a Styrofoam network. Then the shape of the structure can be controlled using the coated Styrofoam spheres. The form can then be debindered and sintered. Cell size can be evenly controlled to sizes in the range of 0.5 – 10 mm and cell wall thickness can be made to 20μm – 1,000 μm. The wall can be sintered fully dense as well as porous.

2.4 Joining Processes

Previous attempts at layering hard stops had been done with limited success using various adhesives. Different joining processes that have the ability to join two dissimilar materials in a permanent manner were researched. The most promising processes were brazing and diffusion welding which are described in further detail in the following sections.

2.4.1 BRAZING

According to the American Welding Society, brazing is a series of welding processes that join two materials via heating and a filler metal that has a liquidous temperature above 840°F (450°C) and below the liquidous temperature of the base materials. There are two methods that are used for bonding the base materials: capillary action and braze welding. Capillary action, in this case, draws the liquid filler metal into the gap between two material surfaces placed on top of each other (10). Braze welding is very similar to the standard welding process where the filler metal is placed at the joint surface and capillary action is not required for the joint to be made. The capillary action process is of most interest in project because of the examination of layered designs. The heat can be provided through several different sources, including furnaces, gas

torches, induction, and resistance. For this project, the gas torch method is the best choice because it is readily available and relatively quick and easy to set up and use.

Brazing could be considered a candidate for materials bonding for several reasons including its versatility in bonding dissimilar materials, and the temperatures reached are generally low, i.e., lower risk of melting / deforming / altering the microstructure of the base materials. The joints are strong, especially in comparison to soldering, are ductile; and have very good vibration resistance. The skills required to properly braze are easily acquired and, especially in the case of the torch method, simply and quickly applied. Materials that can be brazed include: ferrous and nonferrous metals along with their alloys, ceramics, graphite, and diamond.

Various materials have various responses to brazing. The best suited metals are those that do not easily form oxides such as gold, platinum, copper, and cobalt. Those that are in the mid range are refractory metals such as tungsten and molybdenum; those that have good heat and wear resistance, but poor oxidation and corrosion resistance. Metals that have very aggressive oxide layer formation, such as titanium or aluminum, are the hardest to braze. An oxide free surface must be created in order to ensure proper bonding of the filler metal to the material. For those less reactive metals, physical removal of the oxide layer will be sufficient. For more active metals, additional measures such as fluxes and/or controlled atmospheres are required to remove/prevent oxide layers from forming before/during the brazing process. For ceramics, typically a metal alloy is bonded to the surface to be brazed. Some materials forms oxides easily, such as aluminum, to bond with the nonmetallic surface, and others are typically resistant to oxidation, such as copper.

Filler metals must be selected by application basis. Only certain alloy filler metals can be used for joining two specific materials. Some material combinations cannot be brazed because of this. Appendix A contains a partial list of base material combinations and the suitable filler metal to bond them.

For properly designing a brazed joint, there are several items that must be taken into account. The first consideration is joint design and material selection depending on the desired properties with respect to mechanical, electrical, corrosion resistance, etc. Cleaning of the surfaces is critical; any dirt, oil, etc. will not allow that area to be properly bonded. Determining the need for any fluxes or atmospheric controls is next. The fixture to hold the base materials while they are being brazed is critical; a gap of 0.002" - 0.005" is ideal for the liquid filler metal to be drawn into. The heating method must be determined and temperature as controlled as possible; ideally, the heating temperature will be between 50°F - 100°F above the liquidous temperature of the filler metal. However, there is a very small chance that the properties of the material being bonded may change due to the increased temperature (10).

2.4.2 Diffusion Welding

Diffusion welding, also known as diffusion bonding, is a solid state welding process that involved the bonding of two materials through the use of heat, pressure, time, and a controlled atmosphere. Two faces of the materials to be bonded are placed together under pressure and brought to a temperature within 50% - 70% of the lower melting point of the two materials (11). The pressure applied must be sufficiently high to cause plastic deformation at the contacting surface to ensure creep of the material to fill the voids between the two surfaces; it is typically close to the yield stress of the material. Over the course of a predetermined time, atoms from

each material diffuse across the interface and close all gaps that were present upon initial mating. The result is a bond that has similar mechanical properties to those of the base materials.

There are several characteristics of diffusion welding that make it a process of particular interest to this project. It allows for the bonding of dissimilar materials that include metals and ceramics. The joint created, if done properly, has the strength and ductility at least that of the lesser ductile or strong material. Table 14 in Appendix A gives a list of common materials involved in diffusion bonding and their compatibility with each other to form proper joints. There is no additional processing required to clean up the joint after the materials are bonded. Materials with thin oxide layers can be bonded with the prior removal of those layers. Also, there are no dangerous gasses or chemicals involved in the process.

In order to have good bonding, several conditions about the materials and the joining surfaces must be met, in addition to their initial compatibility. Some joints require a thin layer of filler metal to bond, which can be either an actual insert or plating on the joining surfaces. The joining surfaces must be very clean and free of oil, dirt, etc. The ideal surface finish is on the order of 4μm, and any thick layers of oxide will have to be removed. If any one of these conditions is not met, the bond can be far weaker than desired or not occur at all (11).

2.5 Cryogenic Freezing

Cryogenic refers to temperatures that range from -100°C to absolute zero (12). Just as heating a material has effects on its mechanical properties, cryogenically freezing a material also has noticeable effects on a material's properties. The crystalline structure of a metal has a large impact on how it behaves at low temperatures. For example, metals with a body centered cubic

(BCC) structure have a large increase in yield strength at low temperatures, but suffer a loss in ductility. On the other hand, metals with a face centered cubic (FCC) structure typically have a small increase in yield strength, but retain room temperature ductility (12). The retained austenite content of steel can be reduced from 10% (room temperature concentration) to about 3% by cooling it with liquid nitrogen (12). This increases the content of harder martensite in the steel. It is important to understand the effects of cryogenic freezing on a metal because it may have undesired effects on a material, such as a decrease in ductility (e.g. some carbon steels) (12). Cryogenic freezing has also an effect on the strength of adhesives; for example, vinyl and rubber phenolic adhesives typically become weaker at low temperatures, whereas epoxy phenolic and filled epoxide have a small increase in strength (12). The different mechanical properties that result from cryogenic freezing make it an interesting process in this study. An understanding of its effects on various materials and adhesives that can be used to hold layers of different materials together is important to evaluate its acoustic dampening effects.

2.6 Currently Implemented Noise Reduction Technology

Research was done to optimize current methods of noise reduction. Our research was focused on noise dampening technology used in a manufacturing environment. The following sections detail the technology behind several patents on noise reduction.

2.6.1 Anti-Noise Platen

A platen is an element in a machine that is used to make impressions on a media. Platens are used in many types of machines; however, one of the most notable uses is in impact printers. In these machines, platens are flat and typically made of metal (13). Metal is chosen

for its ability to retain shape after many impacts, allowing for accurate manufacture up to tolerance specifications. An invention from 2003 was created with the goal of improving the current noise reduction technology in printing presses. This patented invention proposed that the metal of a platen be imbedded in a plastic body to absorb vibrations and protect the metal (13).

2.6.2 Back Stopper and Damper Plate

As mentioned earlier, the greater the surface area of a part, the louder the noise emanating from it will be. This invention capitalizes on that fact that minimizing the surface area of stopper plate in an impact print head results in less noise emanation and vibration (14). Behind this stopper plate is a damper plate which is specifically engineered to further reduce noise from this machine. The following excerpt from the patent details the structure and materials selection for the back stopper plate:

> "A damper plate made of metal, plastic or rubber, or a laminate of those materials, is placed to the rear of the stopper plate. The best structure is one having outer layers of metal and a middle layer of plastic material. The materials are selected based upon their ability to resist heat and abrasion in addition to having a high damping coefficient." (14)

3 Methodology

A clear and consistent approach to achieving the goals of this project was necessary in order to produce relevant and reliable results. Therefore, there were several key considerations in our methodology to maximize the efficiency and effectiveness of the testing, namely:

- A testing apparatus that as closely as possible replicated the conditions at the sponsor's facility
- Developing prototype hard stops which minimized the variables from prototype to prototype, allowing for a clear interpretation of results
- A data collection procedure which was consistent, repeatable, and reliable.

3.1 Replicating Machine Conditions

In order to accurately test the designed stops, it was important to replicate the actual machine conditions as closely as possible. The first step in this process was to create a solid model of the entire assembly. After creating solid models of all the parts utilizing SolidWorks, the mass can be automatically calculated for all relevant machine parts. In this case, the relevant machine parts are the slide and the hammer. An exploded assembly view can be seen in Figure 3.

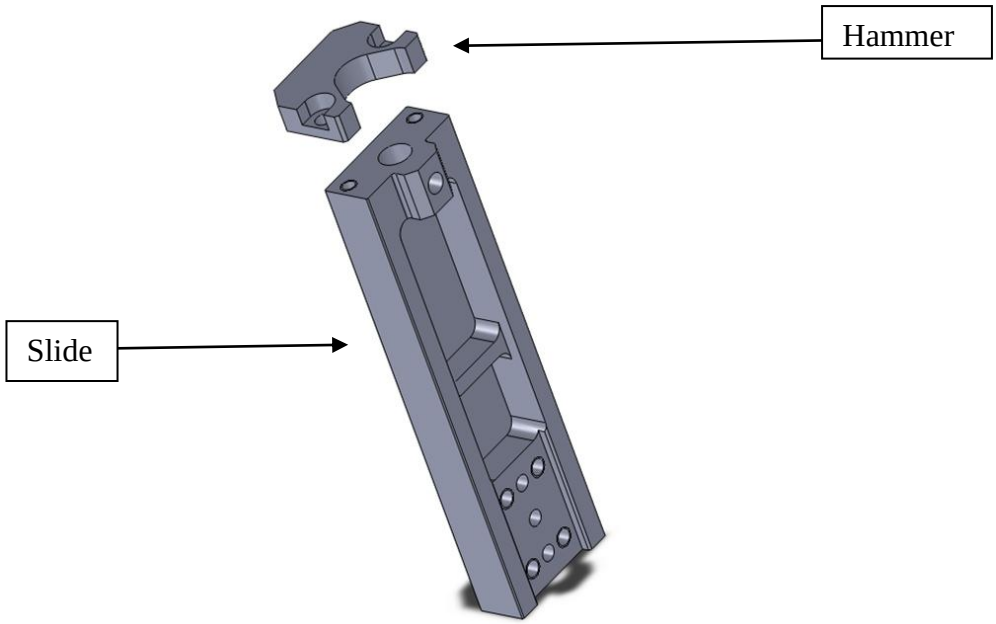

FIGURE 3: SLIDE AND HAMMER EXPLODED ASSEMBLY VIEW.

Once the masses of the moving parts were determined, the acceleration from the tests was used to calculate the impact force of the hammer using $F = m \times a$. This knowledge was found to be very important in this study. A force transducer rated for 500 lbs was used in series with the testing apparatus to feed the impact data to a frequency analyzer. By looking at the power spectrum with the frequency analyzer, it was determined that the impact from the testing apparatus is significantly more than what was measured at the sponsor's location.

In the previous year's team a solenoid hammer was used to conduct testing. This device was housed in a metal box and moved a hardened steel tip on the end of a piston. This piston/hammer device was controlled via a foot pedal to send the electrical signal to actuate the solenoid. The first use of the impact force will be on the piston/hammer testing device used by the previous team to get acoustical data. The machine can have various forces dialed in for the hammer, and when the actual impact force is known, it can be dialed into the acoustical testing device. The end of the piston was eventually modified so that a stop can be mounted to it. The hammer and slide can then be mounted to fixed locations on the same surface or plate as the testing device, and when the piston is activated, the stop is hit against a fixed hammer and slide. Mounting the hammer, slide, and acoustical testing device to the same surface will greatly assist in ensuring consistent conditions for acoustical testing.

3.2 Test Apparatus Design

In order to accurately replicate the condition inside the actual production line machines, a testing apparatus was designed and built. The sponsor provided an assembly of the actual

mechanism that contains the impact stop and hammer. A solid model representation of the assembly is shown below in Figures 4 and 5.

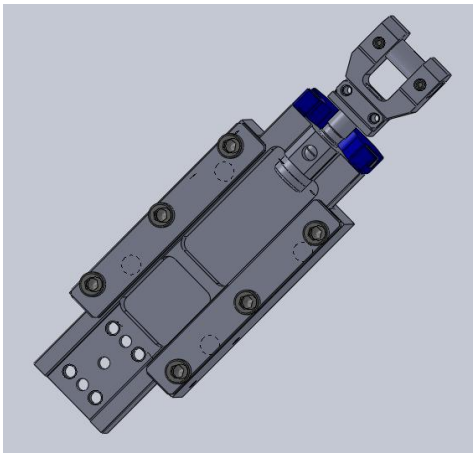

FIGURE 4: SPONSOR-PROVIDED ASSEMBLY.

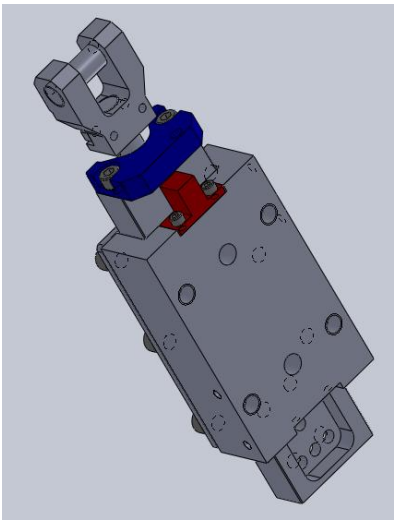

FIGURE 5: ALTERNATE VIEW OF SPONSOR PROVIDED ASSEMBLY.

The primary components of this assembly are the impact stop, highlighted in red, attached to the body through which runs a slide with the hammer attached, highlighted in blue. An exploded assembly view with further detail can be seen in Appendix B. The testing apparatus was constructed after several design iterations. The original design is shown in Figures 6 and 7.

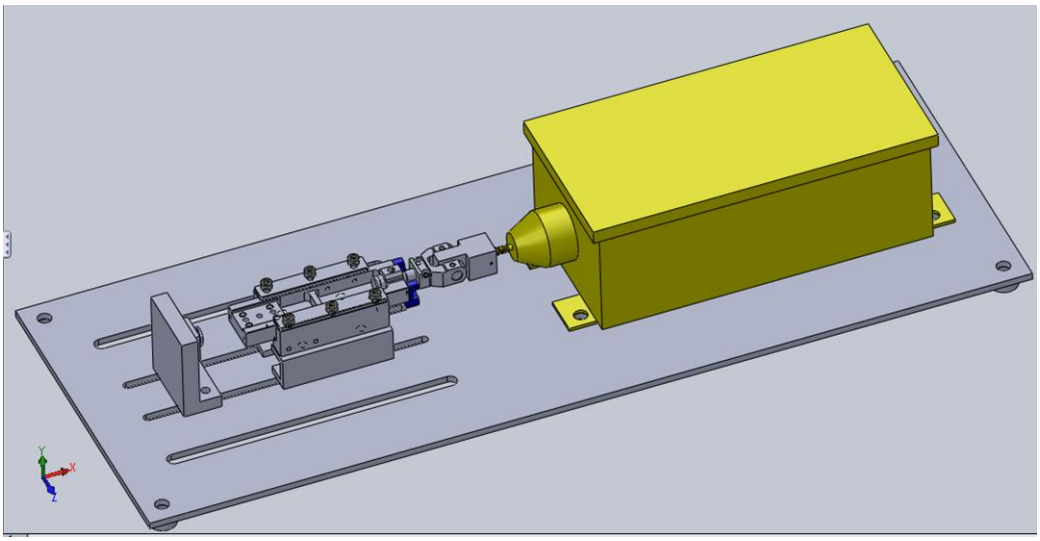

FIGURE 6: REPLICA OF ORIGINAL TEST APPARATUS DESIGN.

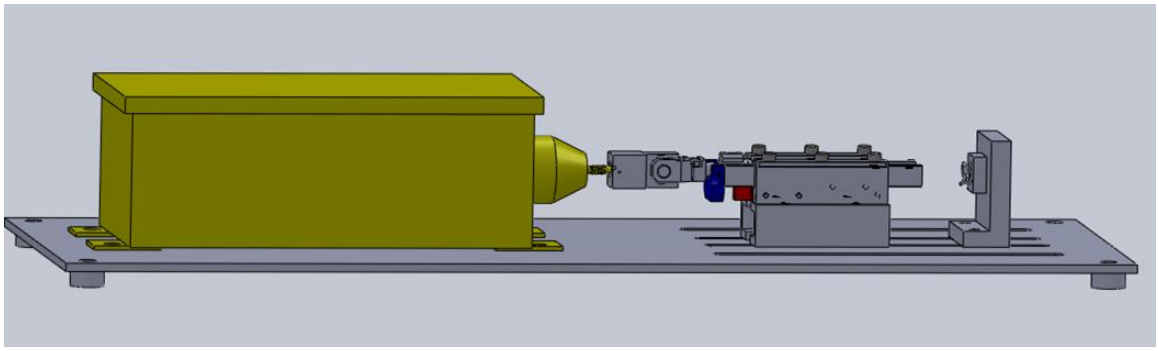

FIGURE 7: ALTERNATE VIEW OF ORIGINAL TEST APPARATUS MOCKUP.

The apparatus was designed to securely hold the sponsor's assembly, an impact hammer, and two force transducers. The original design placed the sponsor's assembly on two pieces of 'c' type channel and had a backing plate with a spring to ensure the slide returned to its original position after every hit. The base plate was created with slots in order to allow for positional adjustment of the equipment for optimal testing conditions and attachment of other equipment, if necessary. The final design, shown in Figures 8 and 9, flips the sponsor's assembly on its side to allow for easy access to the impact stop for observation and quick changeover.

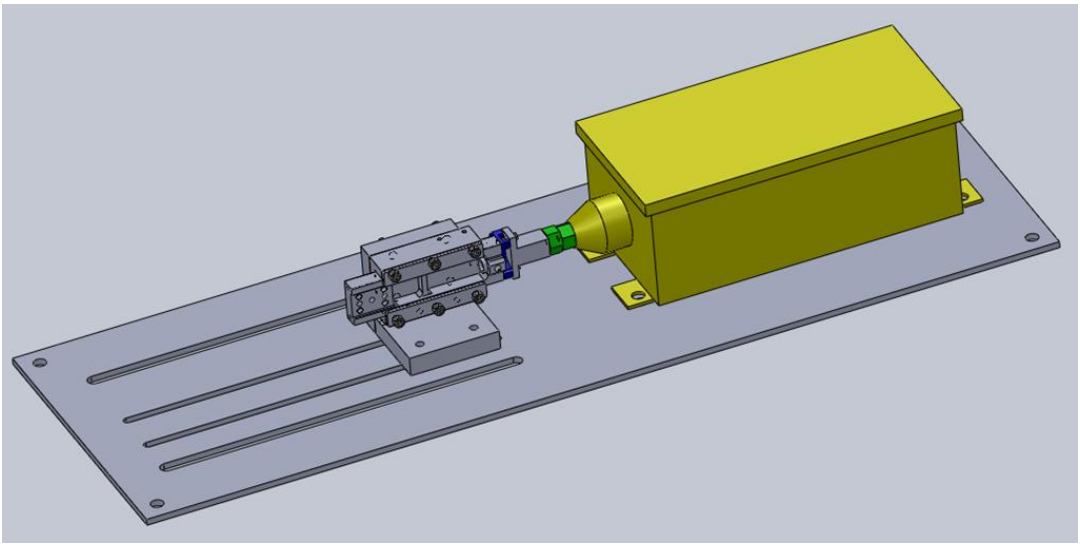

FIGURE 8: FINAL TEST APPARATUS MOCKUP.

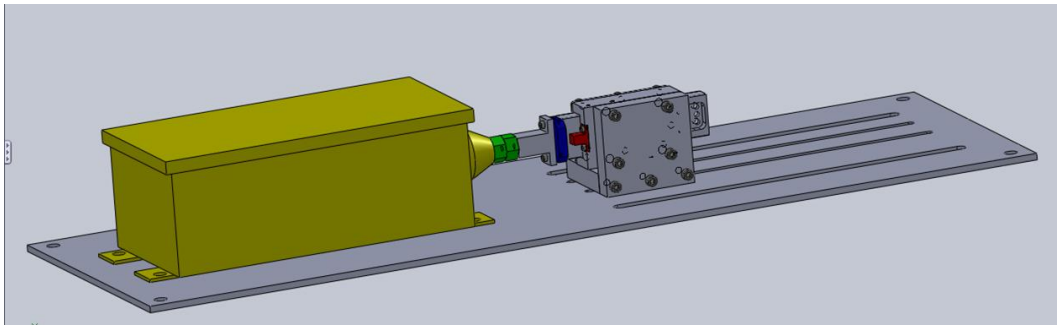

FIGURE 9: ALTERNATE VIEW OF FINAL TEST APPARATUS MOCKUP.

The backing plate was also eliminated in the final design because it was determined that with proper alignment, the impact hammer's internal spring was enough to return the slide to its starting position. The connecting piece between the transducers was modified and the knuckle on the sponsor's assembly was eliminated. It was determined that the original connector created ternary impacts within the system, and reduced the force sent to the impact stop. The powered hammer is highlighted in yellow, force transducers in green, and the final connector in gray, between the transducers and the sponsor's hammer.

3.3 Test Samples

3.3.1 Test Sample Design

Cylindrical samples were designed with a rectangular base and attachment holes placed in the base. The stock base dimensions were used to ensure a proper fit into the actual production mechanism. The choice of a cylindrical impact stop was to maximize the accessible surface area due to virtually no clearance along the back edge of the stop when it is installed in the machine. Figure 10 shows a solid model of a solid prototype stop. These stops were manufactured in once piece from a single material.

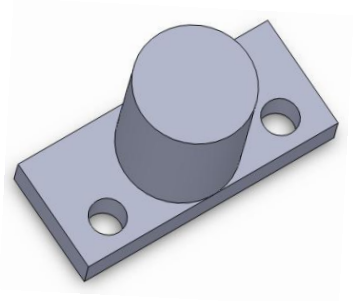

FIGURE 10: PROTOTYPE SOLID STOP.

A coated configuration is shown in Figure 11. The shape is exactly the same as the solid stop, with an additional coating applied to the outside surface of the stop. The model also shows a portion of the coating missing along the back edge of the stop, and this was to allow for clearance of the slide.

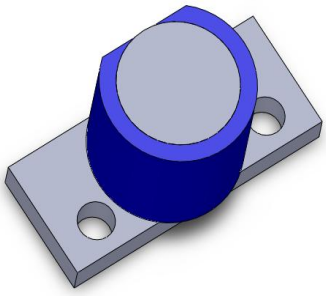

FIGURE 11: PROTOTYPE COATED STOP.

A cored configuration is shown in Figure 12. The shape is the same as the solid stop, but the core of the original structural material was replaced with a dampening material.

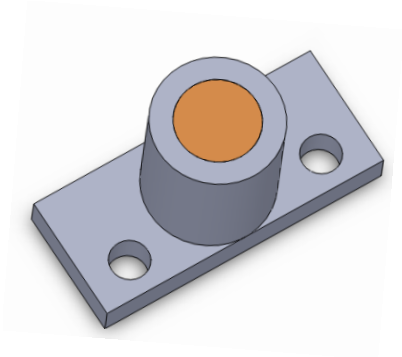

FIGURE 12: PROTOTYPE CORED STOP.

The final prototype stop configuration was a combination of the cored and coated stops discussed above; the solid model is shown in Figure 13.

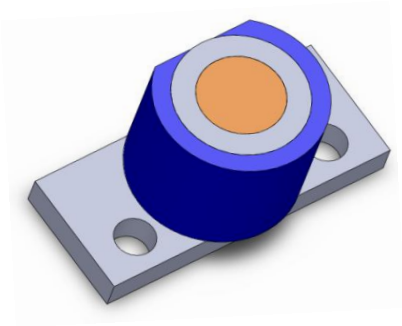

FIGURE 13: PROTOTYPE CORED AND COATED STOP.

Prototype hammers were manufactured using the original geometry, as shown in Figure14, but changing the material.

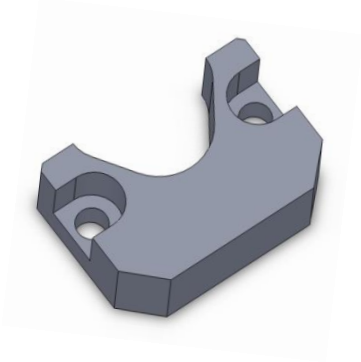

FIGURE 14: PROTOTYPE HAMMER.

3.3.2 Test Sample Manufacture

All prototype stops were manufactured using a two step process, with additional steps for the cored and coated stops. Once the blank was cut and faced, it was fixtured, and the bottom rectangular portion was milled and the holes were drilled. The milled base was then fixtured to mill out the top cylindrical profile. A set of soft jaws were created to fixture each part, while the top profile is milled to allow for damage free clamping and eliminating the need for the use of parallels. Radii were also milled into the soft jaws to fixture the cylindrical stock used for some of the stops, eliminating the need for a machinable collet. For the stops that were coated, the coating was then applied by hand as evenly and as thick as possible to allow for access to the mounting holes and keep the rear of the stop flush with the back edge of the base. For these prototypes with a core, the center of the cylinder was then removed, and if the core was a solid material, a slightly tapered core was milled and press fit.

Prototype hammers were also produced using a two step method. A blank was placed on parallels, and the top profile was milled and the holes were drilled. The part was then turned over, and the bottom faced until the proper height was achieved.

3.4 Material Selection

In order for the impact stop to maintain its structural and dimensional integrity, careful consideration had to be taken when selecting materials for testing. The two mechanical properties that materials were ranked on during the initial material selection were Young's Modulus and Mechanical Loss Coefficient. Young's Modulus was considered because the mechanical stop must be stiff and retain very tight tolerances. Mechanical Loss Coefficient is a

measure of the materials ability to dissipate vibrational energy, and thus, was considered an important material property for this study.

The initial metal groups considered were steels, aluminum alloys, cast irons, and bronzes. After reviewing a case study in the book *Materials Selection in Mechanical Design* by Michael Ashby (15), in which the material selection process was detailed for a stiff, high damping shaker table was detailed (with similar mechanical requirements to the impact stop), and the best material was determined to be a magnesium alloy, magnesium was briefly considered before possible difficulties in manufacturing took it of the materials list. The Granta CES EduPack 2009 software was utilized to create plots ranking materials by selected properties, and was subsequently used to select materials for acoustic testing. Figure 15 shows the materials which were selected and give a reference for how their relevant mechanical properties compare to each others. It should also be noted that 1045 Carbon Steel was used in the study. However, since this material was not available in the Granta database, 1040 Carbon Steel was used for the plot instead of 1045.

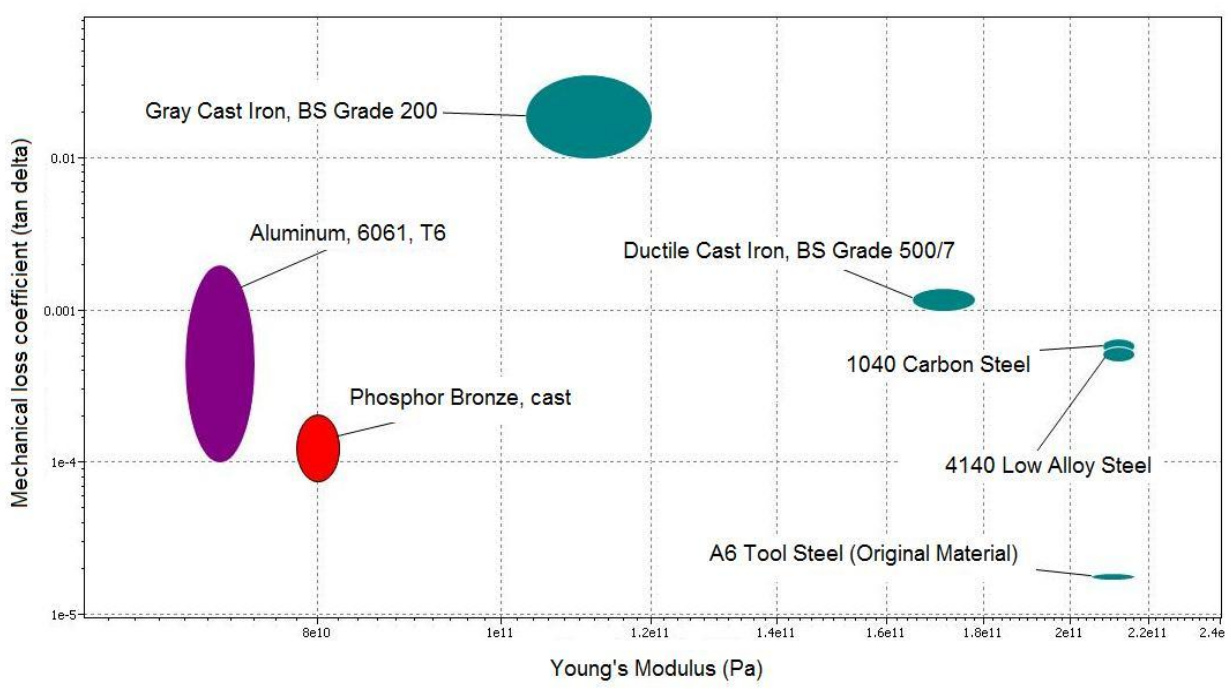

FIGURE 15: MATERIAL SELECTION (MECHANICAL LOSS COEFFICIENT VS. YOUNG'S MODULUS).

An initial review of Figure 15 indicates that the current impact stop material (A6 tool Steel) has one of the lowest mechanical loss coefficients on the graph, meaning that compared to the other selected materials, it has the lowest acoustical dampening. Relevant material properties for these metals are listed in Appendix D. Stops with identical geometry were made from all the materials shown in Figure 15.

In addition to the material properties previously mentioned, the effect of porosity was also investigated. Three different types of bronze were obtained (one cast, one porous PM and one oil-impregnated PM). Like other materials examined, porous bronze was mainly a candidate for filler or damping material, and not a main structural material. These metals were not listed in the CES EduPack software, which is why they are not listed in Figure 15.

3.5 Microstructural Analysis

A thorough microstructural analysis was conducted on all the tested materials. The scope of this analysis was to relate characteristic features of a material's microstructure to the sound readings produced during impact. For extruded materials, part of this analysis was to examine the same material from two different orientations: 1) along the direction of extrusion (longitudinal) and 2) across the direction of extrusions (transverse). The sections below describe the microstructure of the materials used for this project as well as the process used to create these images. Observations relating the microstructures presented in this section will be discussed later in this report.

3.5.1 1045 Carbon Steel

The samples of 1045 carbon steel were prepared by manual grinding with SiC paper down to 600 grit and then automatically polished. After polishing, the samples were etched with 2% Nital to reveal the grains and phases present in the microstructure. Because the samples of 1045 steel were extruded, microstructure was viewed along the axis of extrusion (longitudinal) and across the axis of extrusion (transverse). The optical photos shown in Figures 24-26illustrate microstructure containing two phases: ferrite and pearlite.

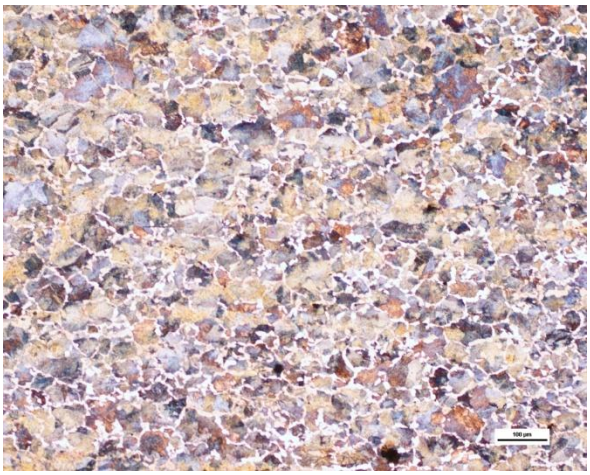

FIGURE 16: 1045 CARBON STEEL: LONGITUDIONAL.

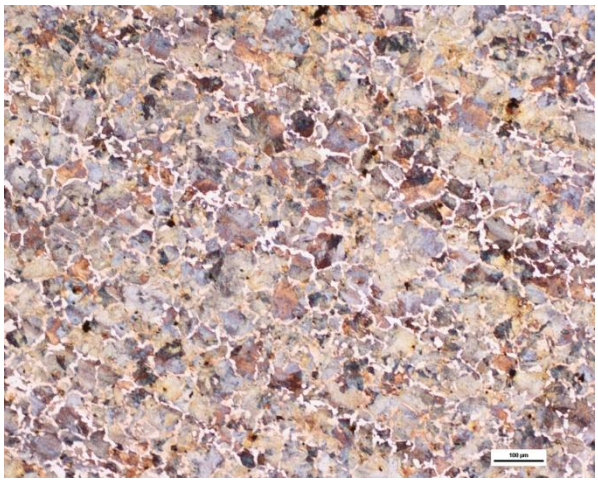

FIGURE 17: 1045 CARBON STEEL: TRANSVERSE.

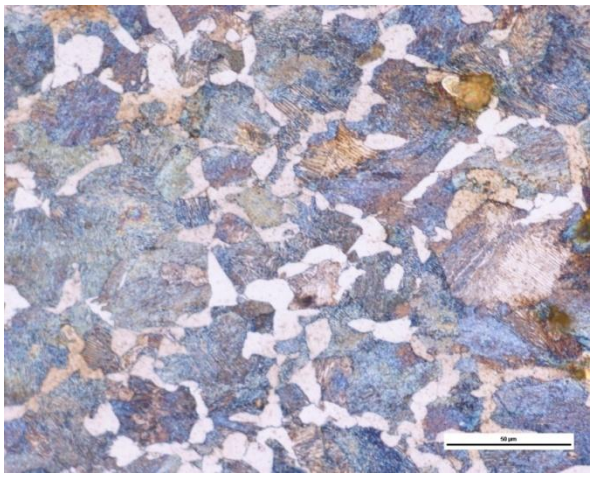

FIGURE 18: 1045 CARBON STEEL: TRANSVERSE.

3.5.2 4140 Low Alloy Steel

The 4140 Low Alloy Steel samples were prepared in the exact same manner as the 1045 Carbon Steel samples. The microstructure of this sample revealed a primarily pearlitic matrix. Darker bands were observed along the axis of extrusion, which were only visible in the transverse direction.

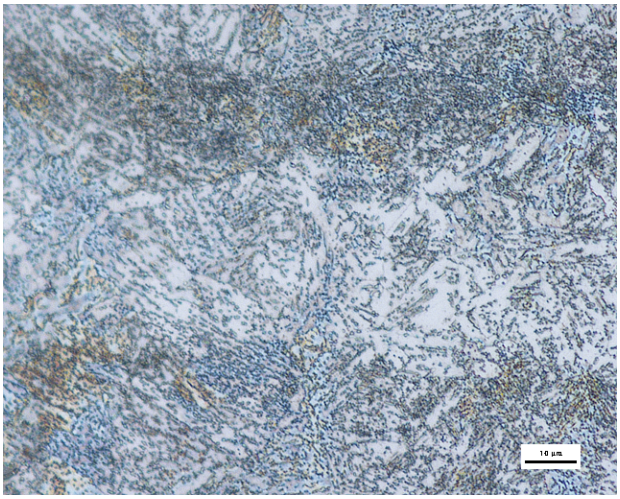

FIGURE 19: 4140 LOW ALLOY STEEL MICROSTRUCTURE: TRANSVERSE.

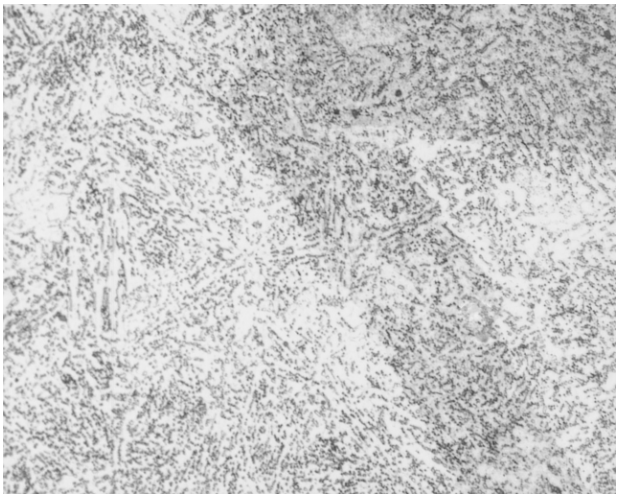

FIGURE 20:4140 LOW ALLOY STEEL MICROSTRUCTURE: LONGITUDIONAL.

3.5.3 GRAY CAST IRON

The gray cast iron samples were prepared by manually grinding down to 600 grit using SiC paper. They were then manually polished and then etched with 2% Nital. In this type of cast iron, the graphite takes the form of flakes which are represented by the black phases embedded in a matrix of pearlite. This material was produced by continuous casting resulting in changes in the size of the graphite flakes based on how close to the center of the original slab the sample was taken from. The closer to the center of the original cast slab, the larger the flakes are.

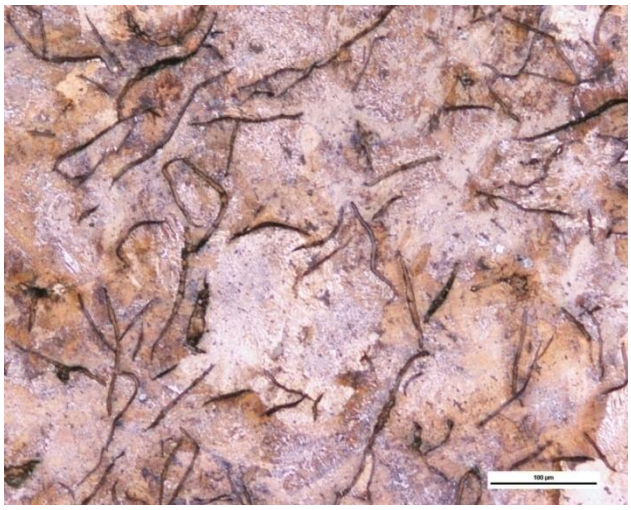

FIGURE 21: GRAY CAST IRON: ETCHED WITH 2% NITAL.

3.5.4 DUCTILE CAST IRON

The samples of ductile cast iron were prepared in the same manner as the gray cast iron discussed earlier. In this type of cast iron, the graphite takes the form of spheres or nodules represented by the black phases in Figure 31. These nodules are embedded in a matrix of ferrite and pearlite. The ferrite is the white colored regions surrounding the nodules, while the pearlite is the darker region between the nodules (which consists of a eutectoid ferrite and cementite).

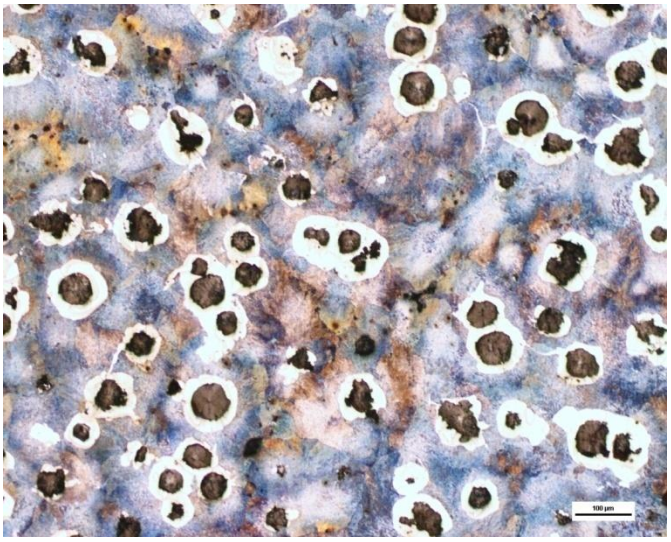

FIGURE 22: DUCTILE CAST IRON: ETCHED WITH 2% NITAL.

3.5.5 PHOSPHOR BRONZE

The cast phosphor bronze was prepared by manually grinding down to 600 grit using SiC paper, and then manually polishing to a mirror shine. The samples were then etched with Curran's reagent revealing a denritic microstructure shown in Figure 32.

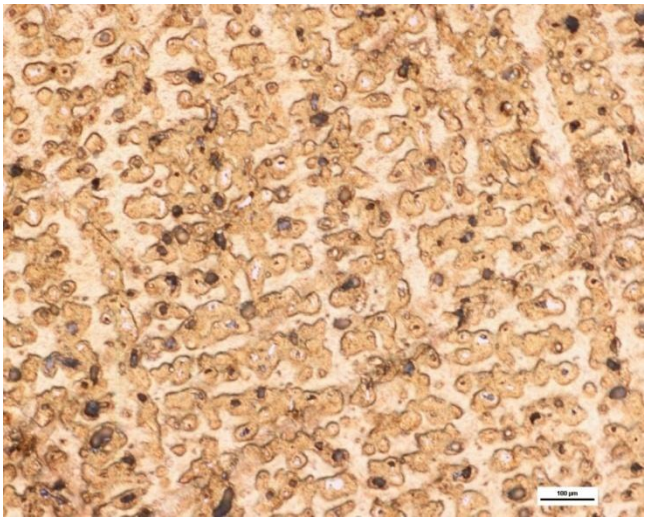

FIGURE 23: PHOSPHOR BRONZE, ETCHED WITH CURRAN'S REAGENT.

3.5.6 Dry Bronze & Oil Impregnated Bronze

The two types of porous materials examined in this study were “dry bronze” and “oil impregnated bronze.” These materials were produced by a powder metallurgy (PM) process resulting in a unique microstructure which is very different from extruded or cast materials. In the “dry bronze” the pores are left as is, which results in small air pockets throughout the material. In “oil impregnated bronze,” oil is sucked through the bronze filling the pores, resulting in oil filed pores. These samples were produced by manually grinding down to 600 grit using SiC paper followed by manual polishing. At this step in the process, the crevices filled with oil or air were visible. However, in order to further reveal the microstructure, the samples were etched with Curran’s reagent, which revealed the particle/grain boundaries.

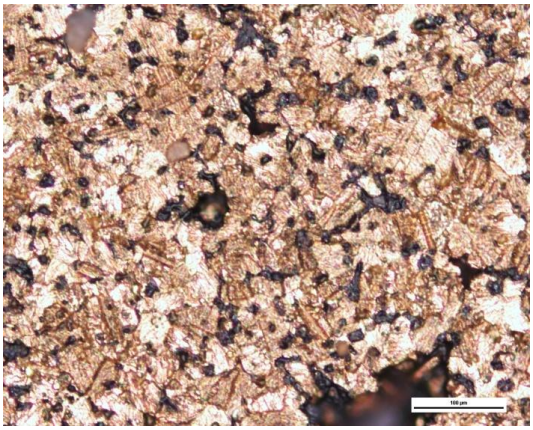

FIGURE 24: POROUS BRONZE: POROUS OIL IMPREGNATED BRONZE.

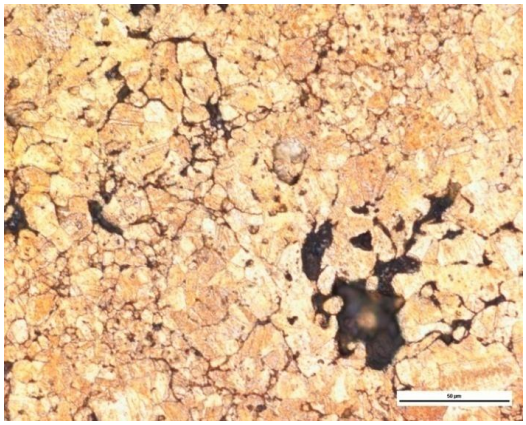

FIGURE 25: POROUS BRONZE: DRY POROUS BRONE.

3.5.7 ALUMINUM 6061

The aluminum alloy that was selected in this project was a 6061 wrought T6 alloy. As with the other materials, the aluminum samples were first manually ground down to 600 grit using SiC paper. Following the grinding, the samples were manually polished. After polishing to a mirror shine, the samples were etched with Keller's Reagent which revealed the grain boundaries. Secondary phases are also visible as the dark spots.

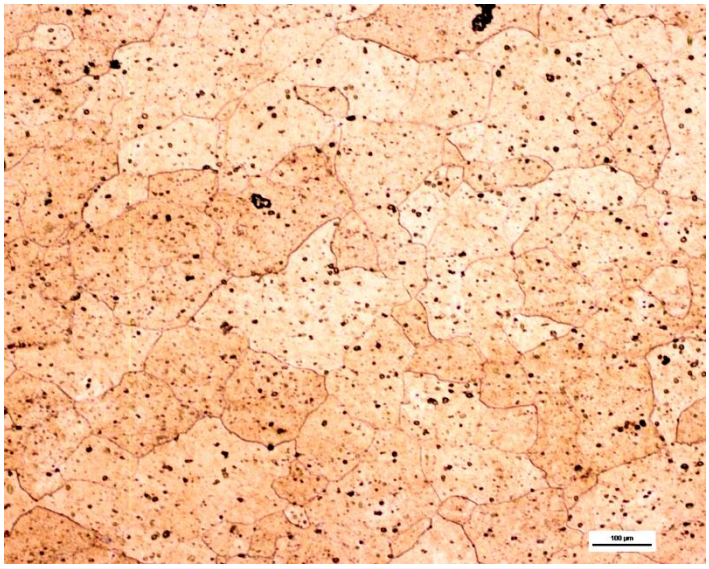

FIGURE 26: ALUMINUM ETCHED WITH KELLER'S REAGENT.

4 RESULTS AND ANALYSIS

4.1 Initial Testing at Sponsor's Location

Testing on the acceleration of the impacting slider, and the sound produced by various materials and configurations of hard stops was conducted at the sponsor's location. The testing was done in the sponsor's maintenance shop, which is a quieter environment than the shop floor; this helped to isolate the test sound from background noise. Samples were produced by the previous year's team, and ground to the required dimensional tolerances before testing. An accelerometer was attached to the moving slide with a magnet. The piezoelectric accelerometer had an excitation current supplied by signal monitor through a mini-coaxial cable. The signal monitor was set up to read acceleration and frequency of the noise produced at the impact site. A Casella sound level meter was placed 6 centimeters from the impact site to record maximum and average sound levels.

Two trials were performed per arrangement to allow for statistical analysis of the results. The standard hard stop was used at several operating speeds to determine the range of expected values for sound readings. All further tests were run at a speed of 200 cycles/minute. This cycle speed was selected because the data acquired from the accelerometer was unreliable at any higher production speed, even though the sound meter still recorded accurate readings. Thirteen different configurations for the hard stop were tested and each configuration was tested twice. Accelerometer data were recorded to a disk as well as read off the signal monitor when the magnitudes of the peaks were determined. The results of the testing are shown in Table 2.

The force was then calculated from the experimentally determined acceleration, and mass of the parts that contribute to the collision with the impact stop. Given the volume of material

derived from the sponsor's drawings of 59.61 cm^3 and the material selected with a density of 7.85 g/m^3, a mass of 0.468 kg was determined for the moving parts. The maximum acceleration measured was 80 times gravitational acceleration, an estimated force of 368 Newtons (82.6 lbf) was found. This was for a sliding configuration without an attachment to do meaningful work, so the mass on a production assembly would be higher. Production settings would likely require higher speeds; therefore, more force must be expected than previously calculated.

4.2 Solid Model Development and Structural Analysis

Before any impact stops were physically machined, solid models of possible designs were created with SolidWorks 2009, and then the Simulation Xpress feature within SolidWorks was utilized to calculate the Factor of Safety (FOS) of each design assuming the force used during our onsite tests at the sponsor's factory and current material (A6 Tool Steel). Solid models were created for seven different stop designs. The seven designs were a standard hard stop, a standard hard stop with a hole, a hard stop with a cylinder, a hard stop with a cored cylinder, a solid block of material, a cylinder, and a cylinder with a hole. Figures 16-22 show the results of the Simulation Xpress analysis on the seven designs. While the factor of safety changes based on the specific material used, these results are helpful because they reveal the strength of the designs relative to each other.

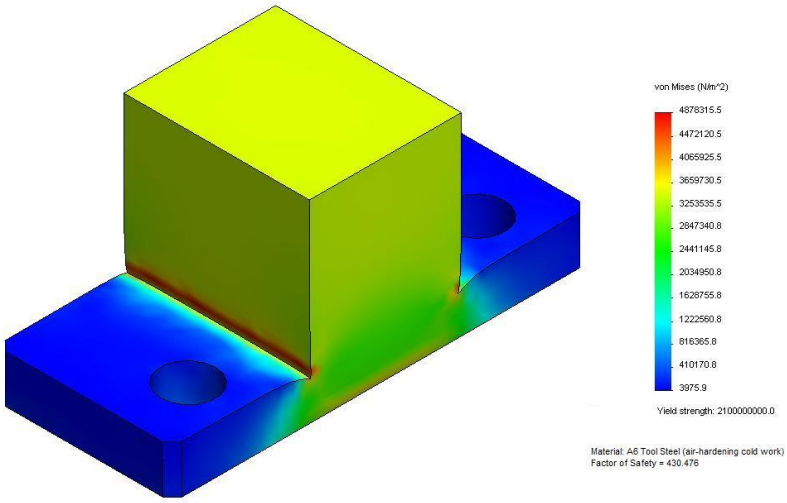

FIGURE 27: STANDARD HARD STOP STRESS DISTRIBUTION.

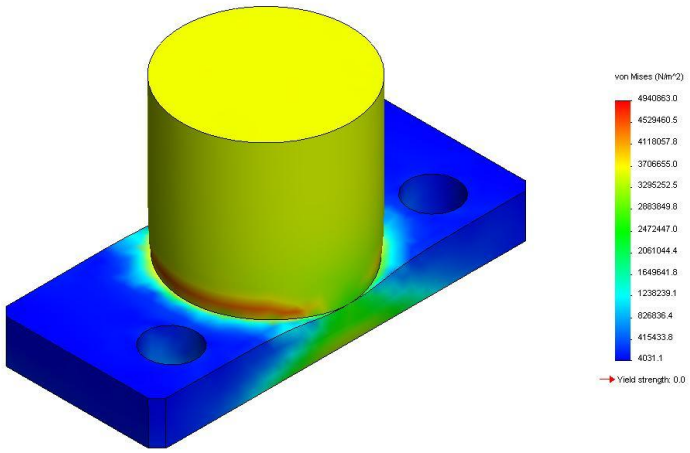

FIGURE 28: PROTOTYPE CYLINDRICAL STOP STRESS DISTRIBUTION.

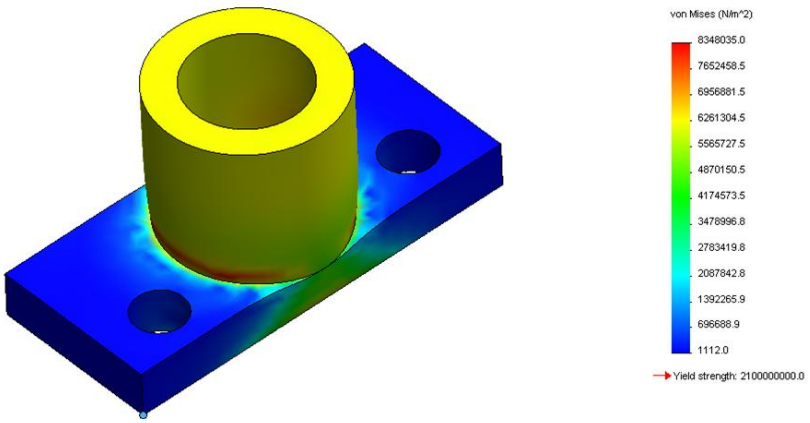

FIGURE 29: PROTOTYPE CYLINDRICAL CORED STOP STRESS DISTRIBUTION.

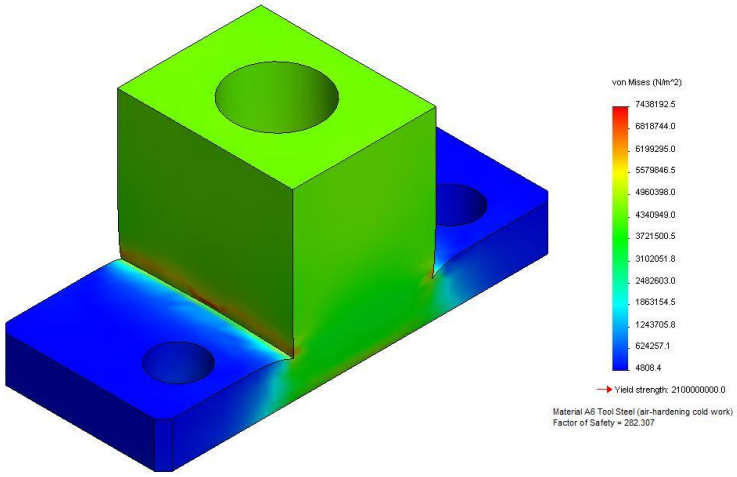

FIGURE 30: STANDARD HARD STOP WITH HOLE STRESS DISTRUBTION.

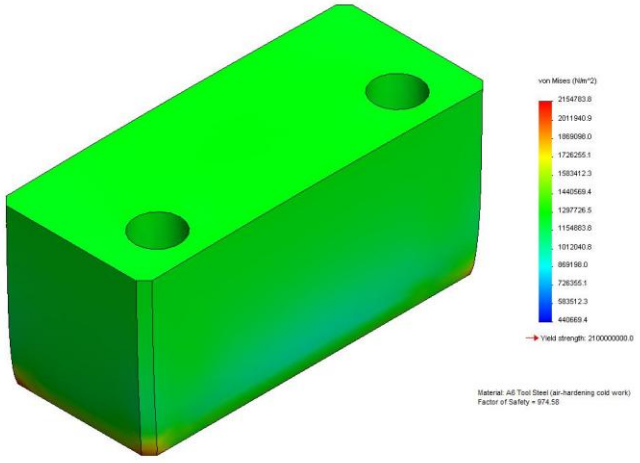

FIGURE 31: SOLID BLOCK HARD STOP STRESS DISTRIBUTION.

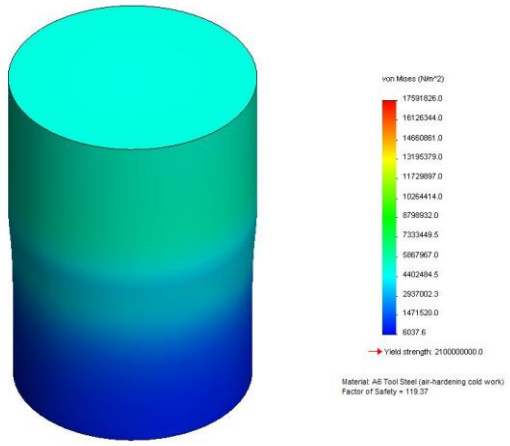

FIGURE 32: CYLINDER HARD STOP STRESS DISTRIBUTION.

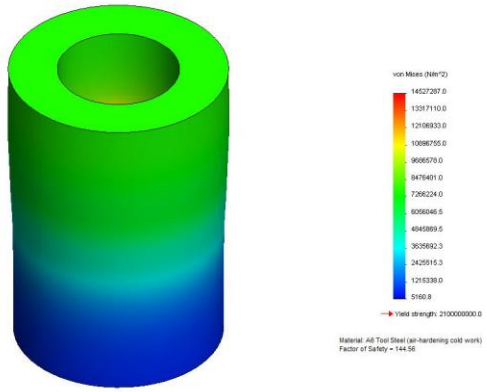

FIGURE 33: CYLINDER HARD STOP WITH HOLE STRESS DISTRIBUTION.

Table 1 details the FOS of each design assuming it was made of A6 Tool Steel and the same force was used during testing. These simulation tests reveal that the stop was a very strong design, which is unlikely to fail under normal circumstances.

TABLE 1: FACTOR OF SAFETY OF HARD STOPS

Design	Factor of Safety
Standard stop	403
Prototype stop with a cylinder	416
Prototype stop with hole	247
Stop with hole	282
Solid block stop	975
Cylinder stop	119
Cylinder stop with hole	145

After the computer simulations were completed, it was decided to have the first set of stops made as hard stops with a cylinder. This decision was made on the similar Factor of Safety to the original design, with both a reduced mass and surface area. Pending the results of the first set of stops, new designs with pugs for damping material would be considered.

4.3 Testing Results from Previous Team's Samples Generated at the Sponsor's Location

Samples made of ductile cast iron, gray flake cast iron, 4140 steel, and 1045 steel were made with cylindrical profiles and flanges for attaching via screws to the assembly. A solenoid hammer actuated via a foot pedal was connected to 2 force transducers by a threaded connector. The solenoid has a dial labeled from 1 to 10 to indicate power of the stroke. The assembly, that is exactly identical to parts used for production at the sponsor's facilities, is mounts on aluminum plates in line with the solenoid. Washers were placed under the sliding block to adjust the height of all parts to achieve the least resistance to movement.

Testing was done at the sponsor's location using a Casella CEL-6X0 series sound level meter. The testing at WPI was conducted using a PCB force transducer rated for 5 volts and 500

lbs, and NDT-RAM software, and the same sound meter used during the testing at the sponsor's location.

TABLE 2: PRELIMINARY TEST DATA

Sample	Average Sound Level (dB)	Average Peak Sound Level(dB)	Average Acceleration (G's)	Average Change in Sound Level (dB)	Standard Deviation
Standard Hard Stop	87.00	114.05	68.17	0.00	0.14
6 (ceramic peg and base plate)	85.30	110.95	62.90	-1.70	0.28
Titanium	87.00	113.55	72.25	1.30	0.14
Al 6061 (solid)	87.30	113.85	70.79	0.30	0.00
Al 6061 (rounded top)	87.35	114.65	73.99	0.350	0.07
11	86.95	114.35	72.44	-0.05	0.07
Cast Iron (rounded top)	87.20	114.15	74.13	0.20	0.14
Cast Iron (3 layer)	87.20	114.35	72.35	0.20	0.00
Al 380 (3 layer)	87.35	116.05	71.69	0.35	0.07
9	85.85	113.25	78.26	-1.15	0.07
10	86.90	114.70	76.05	-0.10	0.00
7	87.05	114.10	68.95	0.20	0.14
Soldered NH or HN	87.05	114.95	71.97	0.05	0.21
3 (large block)	86.70	115.10	73.66	-0.30	0.00
Standard Hard Stop	87.45	115.30	71.73	0.50	0.07

Results from the preliminary tests were compared against the original impact stop data, shown in Table 2. The difference between the results of the test sample and that of the stock impact stop were compared to the standard deviation of the stock impact stop. If the differences in the readings were greater than three standard deviations of the original impact stop the sample was considered to have results statistically significant.

A few of the samples have shown encouraging trends that require more investigation to further improve acoustic performance. A ceramic peg composed of fluorphlogite mica in a borosilicate glass matrix (trade named Macor) placed in the middle of the standard A6 hardened tool steel with a base plate made of aluminum showed the most dramatic improvement of noise reduction with a reduction in sound level of 1.7 dB. A 4 layer configuration composed of A6 tool steel and

Al cast 380 alloy also showed promise with a reduction of 1.15 dB. A block cast iron has shown that an enlarged stop may perform slightly better than the shape currently used for the hard stop. This may be due to a larger surface area to distribute the impact load over. Based on the current research, this result was unexpected, and was investigated further. This is also exemplified with the two samples of cast iron and Al 6061 with rounded top. Both of these samples performed statistically insignificantly different from their flat topped counterparts.

4.4 Testing Results on the New Materials Generated at WPI

Testing was initially done on cylindrical hard stops composed of individual materials to evaluate which material is best suited for further testing with the cored. After analysis of the results was conducted it was determined that the validity of the results was in question due to the appearance of the decibel output trending upward at a constant rate over time, with one exception a 4140 steel sample. The graph of the results from this test, including the trendline that showed the testing apparatus may have been acting inconsistently, is shown in Table 3 and Figure 23. The red data point in Figure 23 represents the 4140 steel stop which broke the otherwise increasing trend in sound output. This information led to choosing it as the material/structure for all future cored prototypes.

TABLE 3: PRELIMINARY TESTING RESULTS

Prototype Material	dB Output
1045 Steel (longitudinal)	102.20
Gray Cast Iron	102.89
Ductile Cast Iron #1	103.37
Ductile Cast Iron #2	103.24
Ductile Cast Iron #3	103.08
Phosphor Bronze	103.47
Dry Bronze	104.09
Oil Bronze	104.54
4140 Steel (Transverse)	103.27
4140 Steel (Longitudinal) #1	104.13
4140 Steel (Longitudinal) #2	104.80

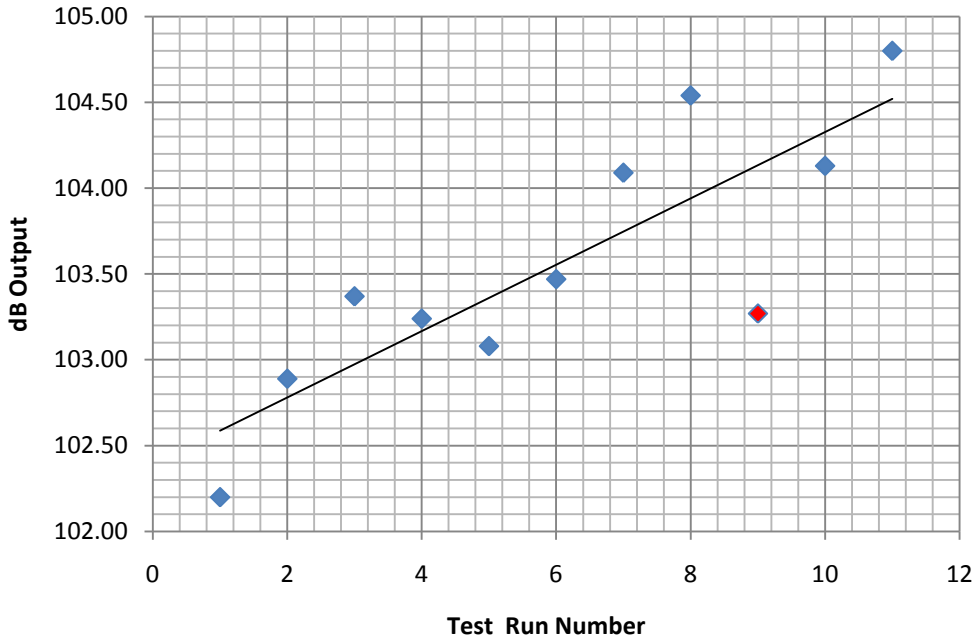

FIGURE 34: PRELIMINARY TESTING RESULTS.

Comprehensive testing was conducted later to prove repeatability of our results. Validated tests were next conducted on all samples with various materials/geometries. The results of these tests are shown in Table 4. Several interesting observations were made. The ductile cast iron is a better candidate for an impact stop than gray cast iron. The carbon content

is similar so the only difference is the microstructure. This implies that nodular graphite phases have better acoustic response upon impact than flakes. It can also be observed that cast bronze responded better than either the dry porous or oil impregnated bronzes due to sound propagation differences through air, oil, and solid metal. Extruded materials showed better damping effects when aligned with the axis of extrusion, likely related to reduced grain boundary area in the direction of the sound wave propagation.

Changes to the material of the hammer were made and led to additional significant decreases in dBA values, with the exception of gray cast iron. Cylindrical samples that were prepared with a core all performed better than the solid cylindrical samples, likely related to the low hardness of the bronze. Samples that were made of a single material but coated with either polyurethane foam or silicone showed noticeable improvements in acoustic damping.

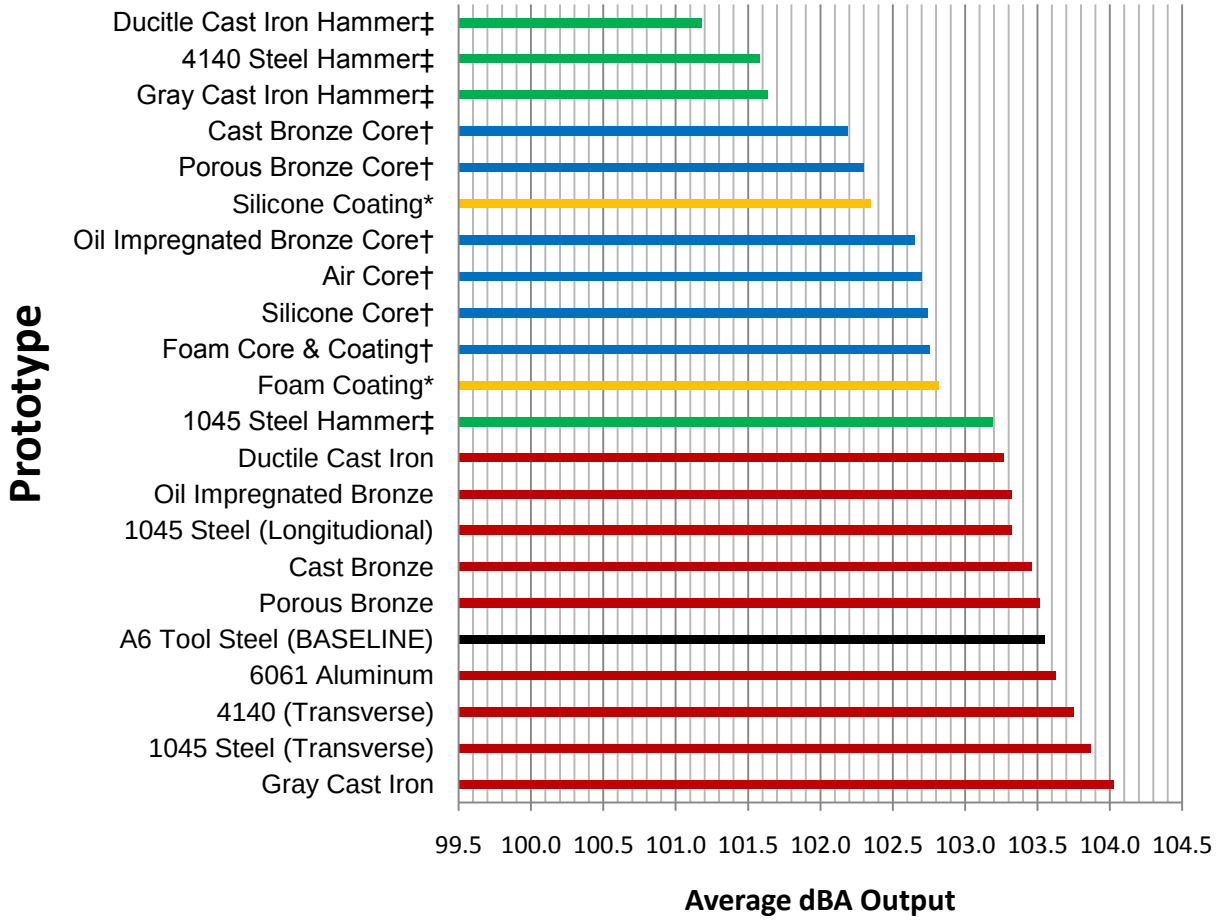

* Coating placed on a 4140 (Longitudinal) prototype
† Structural portion of prototype was made from 4140 (Transverse)
‡ Hammer run with Cast Bronze Core prototype

Key:
Red - Single Material Stop
Orange – Coated Stop
Blue – Cored Stop
Green – Different Hammer Material

FIGURE 35: FINAL RESULTS.

4.5 Microstructural/dBA Output Correlations

Several observations were made about the microstructures of the materials that were tested and their dBA output. Since the two steels tested were manufactured in the form of extruded bars, the grains were elongated along the axis of extrusion. Thus, stops were manufactured with the direction of loading both along and perpendicular to the axis of extrusion.

This means the sound wave encountered a different amount of grain boundary area traveling through these samples. In the case of the 1045 steel, the stop manufactured perpendicular to the extrusion axis performed better by approximately 0.7dBA. A similar trend was observed for the 4140. Literature review has shown that vibrations that turn into sound waves travel easier along grain boundaries than through grains which explain the better performance of the transversal samples (16). The gray and nodular (ductile) cast irons had almost exactly the same wt% composition of carbon and iron, the difference being graphite morphology, thin flakes for the gray cast iron and spherical nodules for the ductile cast iron. The ductile cast iron output was approximately 1.2 dBA lower than that of gray cast iron which indicates the effects of graphite and its morphology on sound. The oil impregnated porous bronze performed approximately 0.2 dBA better than the dry porous bronze. The material and processing were exactly the same in both cases, the only difference being the oil present in the pores of one and air in those of the other. This indicates that oil has a better dampening effect on the vibrations than air.

Developing a relationship between relevant material properties and sound output was one of the goals of this project. After all the data had been collected, various plots were made involving sound output, hardness, Young's Modulus, mass, density, and mechanical loss coefficient. An interesting relation was found between the ratio of Young's Modulus/Hardness and dBA output (i.e. E/Hv vs. dBA). Figure 36 displays the plot, and the trend line illustrates this relationship. The relationship indicates that for a material to have reduced sound output it should have either a low hardness or a high modulus of elasticity. However, it should be noted that in order to further validate this relationship, more data points on various materials are required.

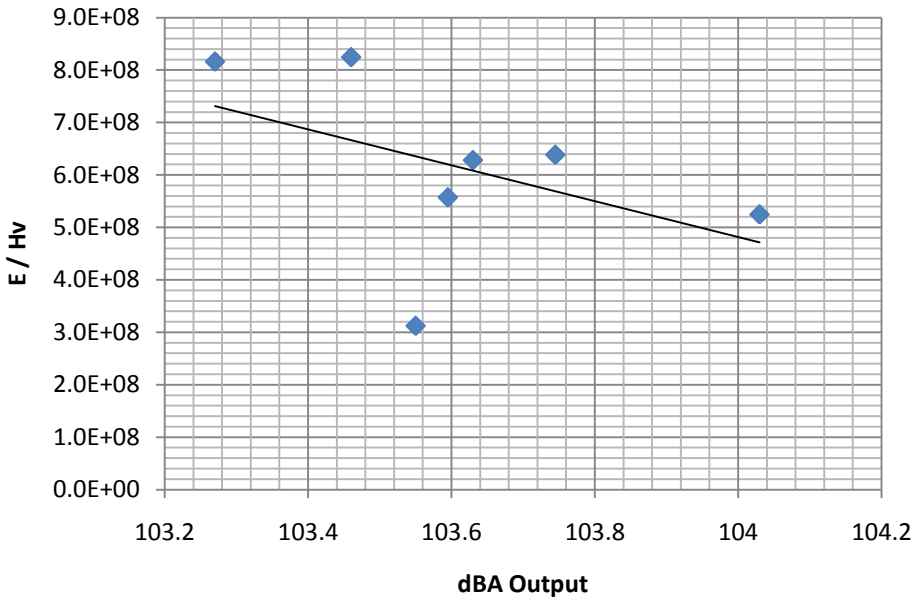

FIGURE 36: SOUND OUTPUT CORRELATION.

5 CONCLUSIONS AND RECOMMENDATIONS

The best results from the battery of testing conducted were produced by the solid bronze cored stop configuration coupled with the nodular cast iron hammer with a reduction of 2.4 dBA over the current stop. An extra dBA was gained simply by changing the material the hammer was made of. As our results have shown, a coating on the hammer is likely to be beneficial as well as a modification in configuration.

Based on our testing and results, microstructure does have an impact on the dBA output of the impacted components as previously discussed. Since our examination was on a broad range of material types and limited samples of each, these microstructural correlations cannot be generalized. It is recommended that a narrower examination of a specific family of materials, i.e., steels, bronzes, etc. is conducted. An even narrower examination of how the differences in microstructure of one material, as a result of different heat treatments, is also recommended.

In the case of nodular versus gray/flake cast irons, the microstructure is the only difference between the two materials. The dBA response of the two had a definite difference in favor of the nodular cast iron, and thus, it can be concluded that the microstructure, namely the graphite morphology, played a role. Further investigation is recommended as to how exactly the two microstructures influence the acoustical output.

For the 1045 steel, a difference was seen between prototype stops manufactured along and across the axis of extrusion, in favor of the longitudinal direction for better sound damping. As our research has indicated, this can be attributed to the lower grain boundary area present in this direction to facilitate sound travel. Further investigation is recommended into the effects of grain boundary area on acoustical output.

In the case of porous bronzes, oil impregnated performed better. Since the only difference between the two materials was that one had pores filled with air and the other with oil, the improved response can be attributed to the presence of the oil. It is recommended that studies will investigate the effects of different materials being placed inside the pores, especially those that have known acoustical dampening characteristics.

The composite stops all had lower dBA output (better dampening characteristics) than the solid configurations. The coupling of a structural material with an experimental dampening core is at the base of the best performing combination. The solid bronze core provided the best response from all materials tested, and further investigation is recommended to understand why, especially since the porous bronzes were favored from previous research. Coatings also enhanced the acoustical dampening although their use was limited during the testing. It is also recommended that evaluation be conducted on a wider variety of core and coating materials.

In order to make the final determination on whether a particular stop and hammer configuration will be suitable, all mechanical requirements must be determined. The load testing conducted at our sponsor's location was on a machine that did not have all the components used in production connected to the slide, which affected our calculations since mass and acceleration were used to equate force. Also, the machine was run at a fraction of the production speed and had a redesigned cam operating mechanism. Taking these three factors into account, it is likely that the forces on the impact stops will be larger during actual production.

Since the top face of the stop will be experiencing rapid, repetitive impacts, a layered stop design is recommended for investigation: a structural material that is able to resist the compressive loading and a material cap with very high fracture and impact toughness. It is

recommended that joining methods such as diffusion bonding, friction stir welding, and brazing be further investigated to join the hard cap to the body of the impact stop. Additionally, a methodical approach (minimizing the number of variables changing in each prototype) to a layered stop design is also recommended.

APPENDIX A: JOINING PROCESSES REFERENCE TABLES

TABLE 4: COMMON BRAZE FILLER METALS

TABLE 25.2 Common Braze Filler Metals in Accordance with AWS A5.8

Filler metal type aluminum	AWS classification	Solidus F	Solidus C	Liquidus F	Liquidus C	Alloy composition Al	Cu	Si	Comments
Aluminum filler metals	BAlSi-3	970	521	1085	585	86	4	10	Aluminum filler metals are used to braze aluminum base metals. Typical base metals joined are the 1100, 3000, and 6000 series aluminum alloys. Aluminum brazing requires tighter process parameters than most brazing processes due to the close relationship between the melting point of the filler metals and base metals.
	BAlSi-4	1070	576	1080	582	88		12	

Filler metal type copper	AWS classification	Solidus F	Solidus C	Liquidus F	Liquidus C	Alloy composition Cu	Comments
Copper filler metals	BCu-1	1981	1083	1981	1083	99.9 Min.	Copper filler metals are primarily used in furnace brazing ferrous base materials such as steels and stainless steels. Note BCu-1 is produced only in wire and strip form. BCu-1a is the powder form of BCu-1.
	BCu-1a	1981	1083	1981	1083	99.0 Min.	

Filler metal type copper	AWS classification	Solidus F	Solidus C	Liquidus F	Liquidus C	Alloy composition Cu	Zn	Sn	Fe	Mn	Ni	Comments
Copper /zinc filler metals	RBCuZn-C	1590	866	1630	888	58	40	0.95	0.75	0.25		The copper/zinc based filler metals are used in joining steels, copper, copper alloys, nickel, nickel alloys, and stainless steels. Heating methods typically used are torch and induction with flux. Due to the high zinc content of these filler metals, they are rarely used in furnace brazing process.
	RBCuZn-D	1690	921	1715	935	48	42				10	

Filler metal type copper	AWS classification	Solidus F	Solidus C	Liquidus F	Liquidus C	Alloy composition Ag	Cu	P	Comments
Copper/phosphorus filler metals	BCuP-2	1310	710	1460	793		92.7	7.3	The copper/phosphorus filler metals are used to braze copper and copper alloys. The can also be used to braze electrical contacts containing cadmium oxide or molybdenum. These filler metals are considered self-fluxing on copper base metals.When used to braze various copper alloys (i.e., brass) a mineral type flux is recommended. Do not use these filler metals on ferrous materials or nickel bearing material in excess of 10% nickel as brittle phosphides will be formed at the braze interface.
	BCuP-3	1190	643	1495	813	5	89	6	
	BCuP-4	1190	643	1325	718	6	86.7	7.3	
	BCuP-5	1190	643	1475	802	15	80	5	

25.5

TABLE 5: COMMON BRAZE FILLER METALS IN ACCORDANCE WITH AWS A5.8

TABLE 25.1 Base Metal-Filler Metal Combinations

	Al & Al alloys	Mg & Mg alloys	Cu & Cu alloys	Carbon & low alloy steels	Cast iron	Stainless steel	Ni & Ni alloys	Ti & Ti alloys	Ba, Zr, & alloys (reactive metals)	W, Mo, Ta, Ch & alloys (refractory metals)	Tool steels
Al & Al Alloys	BAlSi										
Mg & Mg alloys	X	BMg									
Cu & Cu alloys	X	X	BAg, BAu, BCuP, RBCuZn	BNi							
Carbon & low alloy steels	BAlSi	X	BAg, BAu, RBCuZn, BNi	BAg, BAu, BCu, RBCuZn, BNi							
Cast iron	X	X	BAg, BAu, RBCuZn, BNi	BAg, RBCuZn, BNi	BAg, RBCuZn, BNi						
Stainless steel	BAlSi	X	BAg, BAu	BAg, BAu, BCu, BNi	BAg, BAu, BCu, BNi	BAg, BAu, BCu, BNi					
Ni & Ni alloys	X	X	BAg, BAu, RBCuZn, BNi	BAg, BAu, BCu, RBCuZn, BNi	BAg, BCu, RBCuZn	BAg, BAu, BCu, BNi	BAg, BAu, BCu, BNi				
Ti & Ti alloys	BAlSi	X	BAg	BAg	BAg	BAg	BAg	Y			
Be, Zi & alloys (reactive metals)	X BAlSi (Be)	X	BAg	BAg, BNi*	BAg, BNi*	BAg, BNi*	BAg, BNi*	Y	Y		
W, Mo, Ta, Cb & alloys (refractory metals)	X	X	BAg, BNi	BAg, BCu, BNi*	BAg, BCu, BNi*	BAg, BCu, BNi*	BAg, BCu, BNi*	Y	Y	Y	
Tool steels	X	X	BAg, BAu, RBCuZn, BNi	BAg, BAu, BCu, RBCuZn, BNi	BAg, BAu, RBCuZn, BNi	BAg, BAu, BCu, BNi	BAg, BAu, BCu, RBCuZn, BNi	X	X	X	BAg, BAu, BCu, RBCuZn, BNi

Note: Refer to AWS Specification A5.8 for information on the specific compositions within each classification.
X—Not recommended; however, special techniques may be practicable for certain dissimilar metal combinations.
Y—Generalizations on these combinations cannot be made. Refer to the Brazing Handbook for usable filler metals.
*—Special brazing filler metals are available and are used successfully for specific metal combinations.

Filler Metals:
BAlSi—Aluminum
BAg—Silver base
BAu—Gold base
BCu—Copper
BCuP—Copper phosphorus
RBCuZn—Copper zinc
BMg—Magnesium base
BNi—Nickel base

TABLE 6: COMMON BRAZE FILLER METALS IN ACCORDANCE WITH AWS A5.8 (CONTINUED)

TABLE 25.2 Common Braze Filler Metals in Accordance with AWS A5.8 (*Continued*)

Filler metal type silver	AWS classification	Solidus F	Solidus C	Liquidus F	Liquidus C	Alloy composition Ag	Cu	Zn	Cd	Sn	Ni	Comments
Cadmium bearing silver filler metals	BAg-1	1125	607	1145	618	45	15	16	24			Silver based filler metals can be used to braze a variety of base materials. In general all ferrous and non-ferrous base materials can be joined. Note that the temperature range of the liquidus temperatures of the silver based filler metals (1145°F to 1761°F) preclude them from being used to join aluminum or magnesium. This large temperature range for the silver group provides for a selection of filler metals to be utilized in brazing at the lowest temperature, or brazing at a temperature in which heat treated properties may be obtained in the base materials. Silver based filler metals can be used by all heating methods; however, when choosing a filler metal to be used in an atmosphere or vacuum process, the content of the filler metal should not contain cadmium or zinc. Cadmium and zinc can volitalize from the filler metal contaminating the work and/or furnace. Silver filler metals that contain cadmium as a principal constituent require care to avoid exposure to cadmium fumes. Filler metals which contain 1% to 5% nickel are found to be efffective in wetting carbide materials. They will also inhibit or prevent interface corrosion on stainless steels.
	BAg-2	1125	607	1295	701	35	26	21	18			
	BAg-3	1170	632	1270	687	50	15.5	15.5	16		3	
Cadmium free silver filler metals	BAg-4	1240	670	1435	779	40	30	28			2	
	BAg-5	1225	662	1370	743	45	30	25				
	BAg-7	1145	618	1205	651	56	22	17		5		
	BAg-13	1325	718	1575	856	54	40	5			1	
	BAg-13a	1420	770	1640	892	56	42				2	
	BAg-21	1275	690	1475	801	63	28.5			6	2.5	
	BAg-24	1220	659	1305	707	50	20	28			2	
	BAg-28	1200	648	1310	709	40	30	28		2		
	BAg-34	1200	648	1330	720	38	32	28		2		
	BAg-36	1195	643	1251	677	45	27	25		3		
	BVAg-8Gr2	1435	779	1435	779	72	28					
	BVAg18Gr2	1115	601	1325	718	60	30			10		
	BVAg29Gr2	1155	623	1305	707	61.5	24			14.5		

Filler metal type gold	AWS classification	Solidus F	Solidus C	Liquidus F	Liquidus C	Alloy composition Ag	Au	Cu	Pd	Ni	Comments
Gold filler metals	BAu-1	1815	991	1860	1016		37.5	62.5			Gold based filler metals are used to join steels, stainless steel, nickel based alloys, where ductility and resistance to oxidation or corrosion is required. Gold filler metals readily wet most base materials including super alloys and are especially good for brazing thin sections due to their low interaction with most base materials. Most gold based filler metals are rated for continuous service up to 800°F. Gold filler metals are typically brazed in either a protective atmosphere or vacuum process.
	BAu-3	1785	974	1885	1029		35	62		3	
	BVAu-4	1740	949	1740	949		82			18	
	BAu-6	1845	1007	1915	1046		70		8	22	
	BVAu-8	2192	1200	2264	1240		92		8		

TABLE 7: COMMON BRAZE FILLER METALS IN ACCORDANCE WITH AWS A5.8 (CONTINUED)

Filler metal type nickel	AWS classification	Solidus F	Solidus C	Liquidus F	Liquidus C	Alloy composition Ni	Cr	Si	B	Fe	P	Comments
Nickel filler metals	BNi-1	1790	977	1900	1038	73.1	14	4	3.1	4.5		Nickel based filler metals are used to braze ferrous and non-ferrous, high temperature base materials, such as stainless steels and nickel based alloys. These filler metals are generally used for their strength, high temperature properties, and resistance to corrosion. Some of these filler metals can be used in continous service up to 1800°F (980°C), and 2200°F (1205°C) for short periods of time. Nickel base filler metals melt in the range of 1610°F (C) to 2200°F (C) but can be used at higher temperatures when the melting depressant elements in the filler metal such as silicon and boron are diffused from the filler metal into the base maetal altering the composition of the joint.
	BNi-2	1780	971	1830	999	82.3	7	4.5	3.1	3		
	BNi-6	1610	877	1610	877	89					11	
	BNi-7	1630	888	1630	888	75.9	14				10.1	

For more information on the filler metal types above, or BCo, BMg, BPd refer to the American Welding Societies "Specification for Filler Metals for Brazing and Braze Welding."

TABLE 8: DIFFUSION WELDING COMBINATIONS OF METALS AND ALLOYS

Table 33.6 DIFFUSION WELDING COMBINATIONS OF METALS AND ALLOYS WITHOUT AN INTERLAYER (DIRECT) AND WITH AN INTERLAYER (INDIRECT)*

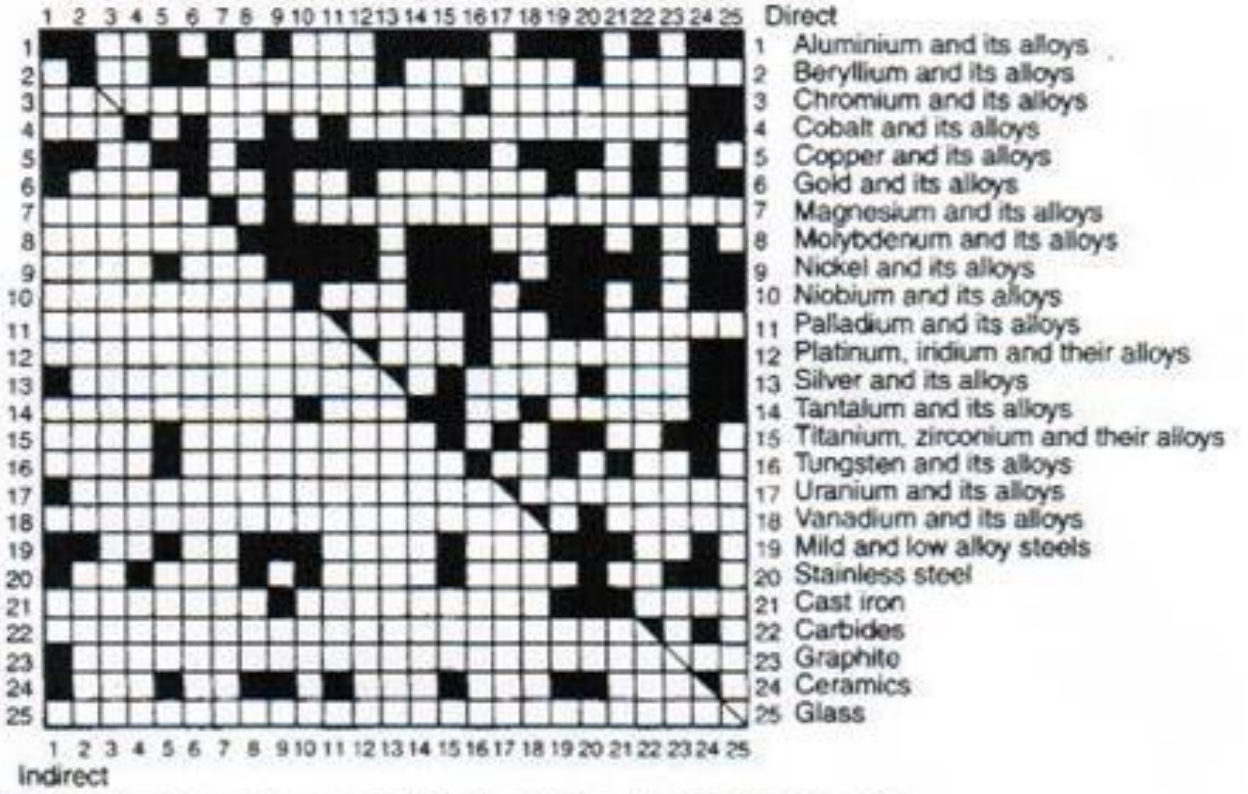

* For further information, *see* P. M. Bartle, *Welding J.*, 1975, **54**, 799–804.

APPENDIX B: SOLID MODEL ASSEMBLIES

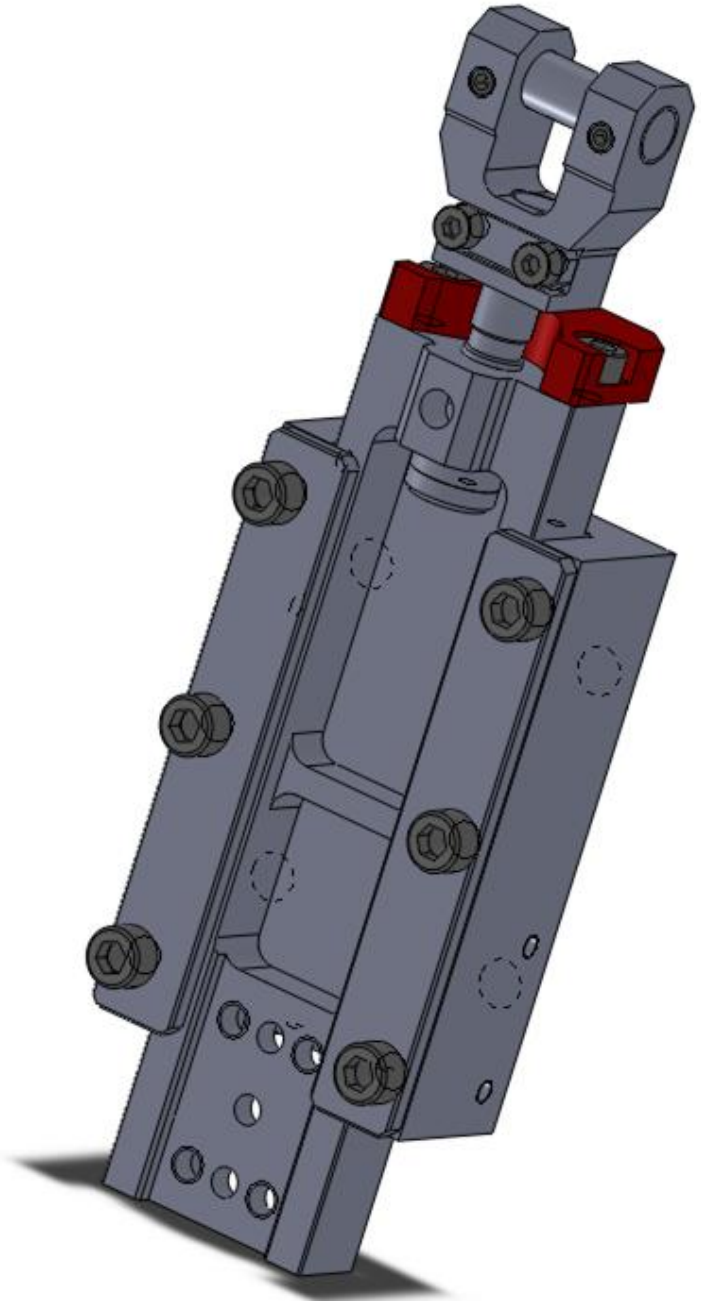

FIGURE 37: SPONSORS'S MECHANISM ASSEMBLY REAR VIEW.

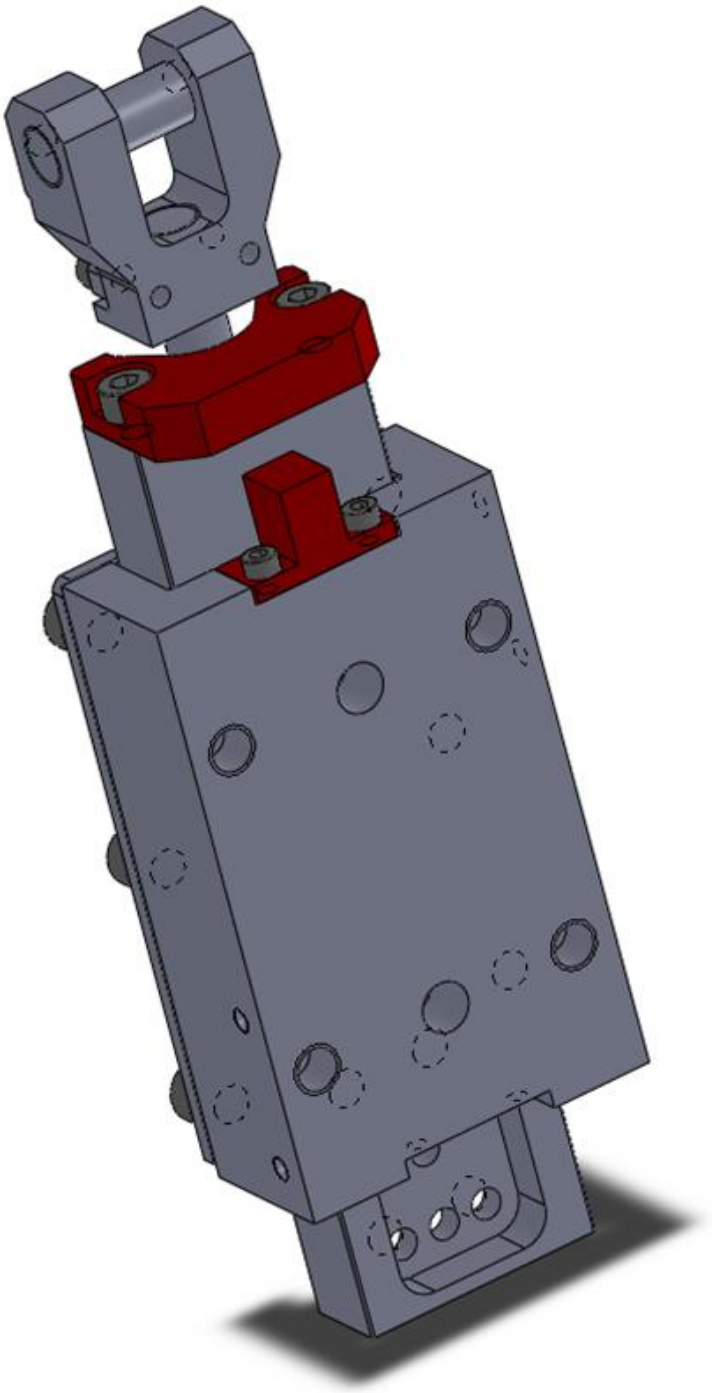

FIGURE 38: SPONSOR'S MECHANISM ASSEMBLY FRONT VIEW.

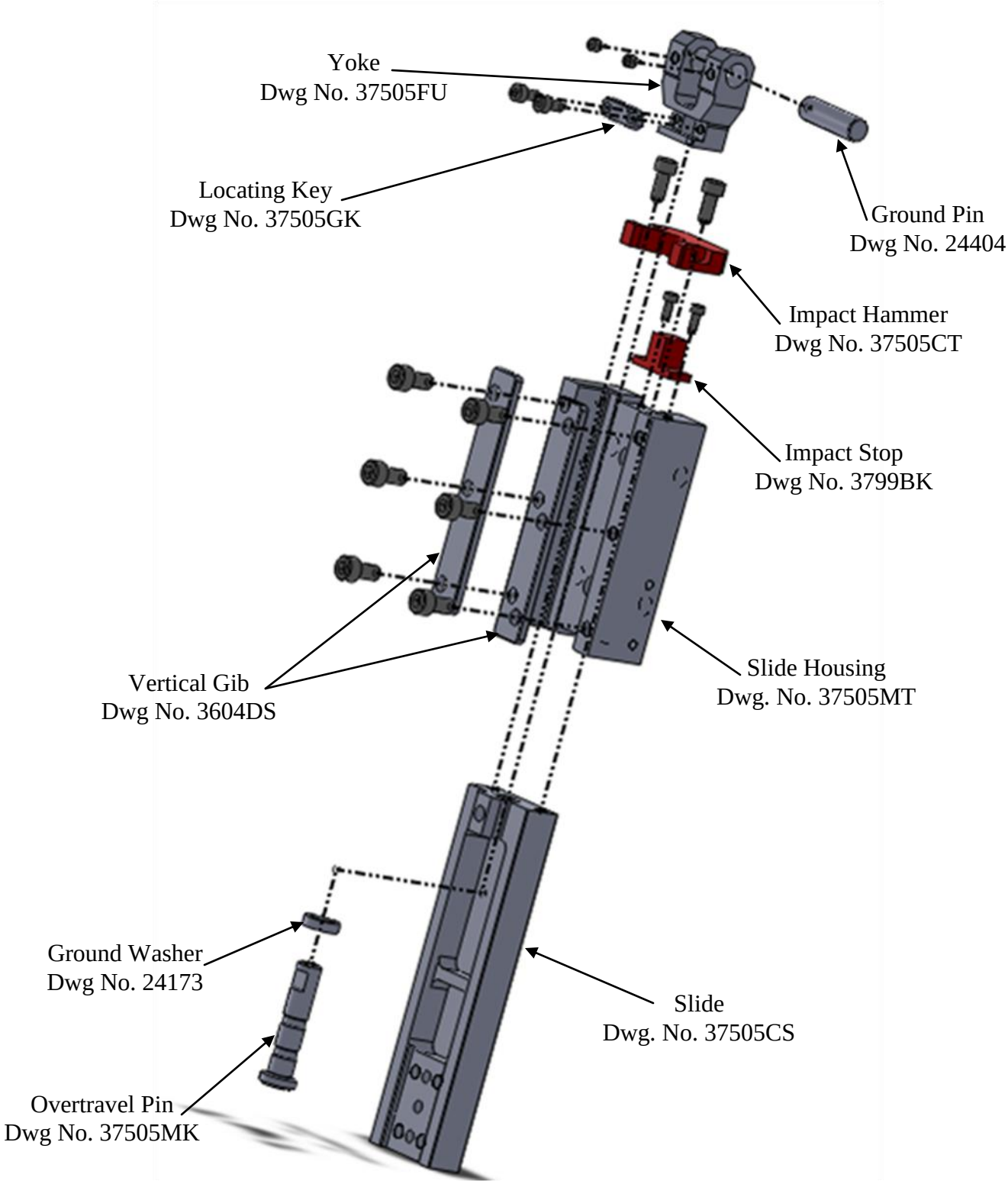

FIGURE 39: SPONSOR'S MECHANISM EXPLODED ASSMEBLY VIEW WITH DRAWING DESIGNATIONS.

APPENDIX C: ETCHANTS

TABLE 9: ETCHANTS

Etchant	Components	Materials Etched
2% Nital	2ml Nitric Acid ($HN0_3$) & 98ml Ethyl Alcohol	1045 Carbon Steel, 4140 Low Alloy Steel, Gray Cast Iron, & Ductile Cast Iron
Curran's Reagent	10g Ferric Chloride ($FeCl_3$), 30ml Hydrochloric Acid (HCl), & 120ml Water (H_2O)	Porous Bronze, Dry Bronze, & Oil Impregnated Bronze
Keller's Reagent	2.5ml Nitric Acid (HNO3), 1.5ml Hydrochloric Acid (HCl), 1ml Hydrofluoric Acid (HF), & 95ml Water (H2O)	Aluminum 6061

APPENDIX D: RELEVANT MATERIAL PROPERTIES AND PROCESSING

The following table lists the material properties of metals which were pertinent to this project. The hardness, average mass of a solid prototype, and sound output values were obtained during testing and the remaining properties were obtained with the assistance of Granta software.

TABLE 10: MATERIAL PROPERTIES AND PROCESSING

Material	Mechanical Loss Coefficient (tan delta)	Young's Modulus (Pa)	Yield Strength (Pa)	Hardness (HV)†	Average mass of solid prototype (g)	Processing and Heat Treatment	Sound output (dBA)
1045 Steel	5.85E-04	2.12E+11	6.33E+08	380.4	15.23	Extruded, Tempered at 425°C & H2O quenched	103.60
4140 Steel	5.15E-04	2.12E+11	6.55E+08	332.0	15.54	Extruded, Normalized	103.75
Gray Flake Cast Iron	2.25E-02	1.11E+11	1.37E+08	211.5	14.03	Continuously Cast	104.03
Ductile Cast Iron	1.20E-03	1.71E+11	3.56E+08	209.5	13.95	Continuously Cast	103.27
Phosphor Bronze	1.40E-04	8.00E+10	1.85E+08	97.0	17.34	Cast	103.46
Aluminum 6061	1.05E-03	7.10E+10	2.42E+08	113.0	5.05	Wrought, T6	103.63
A6 Tool Steel	3.56E-05	2.11E+11	2.10E+09	674.0	15.44	Air-hardened	103.55
Dry Bronze	*	*	*	*	11.92	Powder Metallurgy	103.52
Oil Bronze	*	*	*	*	11.96	Powder Metallurgy	103.32

Note: * indicates material properties not obtained in Granta or during testing.

† indicates that the hardness readings were originally calculated in a Rockwell a scale and then converted to Vickers.

REFERENCES

1. Noise Induced Hearing Loss. *Hearing Loss Web.* [Online] 2010. [Cited: April 18, 2010.] http://www.hearinglossweb.com/Medical/Causes/nihl/nihl.htm.

2. **Penton Media, Inc.** Sound Absorbing Material - A Quick Guide. *Mix Professional Sound Audio and Music Production.* [Online] [Cited: October 6, 2009.] http://mixonline.com/online_extras/sound_absorbing_materials/.

3. *Calculation of Sound Absorption Characteristics of Porous Sintered Metal.* **Bo, Zhang and Tianning, Chen.** 2007, Applied Acoustics.

4. **Fomo Products, Inc.** Open-cell vs. Closed-cell. *Fomo Products, Inc.* [Online] 2008. [Cited: October 06, 2009.] http://www.fomo.com/resources/technical-bulletins/opencellvsclosed.aspx.

5. **Global Urethane Services pty ltd.** Polyurethane Spray Sound Absorption Foam. *Global Urethane Services.* [Online] [Cited: October 06, 2009.] http://www.global-urethane-and-sealing-services.com/sound-absorption-foam.html.

6. A-weighting in detail. *Lindos Electronics.* [Online] [Cited: March 6, 2010.] http://www.lindos.co.uk/cgi-bin/FlexiData.cgi?SOURCE=Articles&VIEW=full&id=2.

7. *New Multifunctional Lightweight Materials Based on Cellular Metals - Manufacturing, Properties, and Applications.* **Stephani, Gunter, Quadbeck, Peter and Olaf, Andersen.** 2009, Journal of Physics: Conference Series 165.

8. **Li, C., et al.** *Sound Absorption Characters of Metal Fibrous Porous Material.* 2007.

9. *Metal Foaming by a Powder Metallurgy Method: Production, Properties and Applications.* **Chin-Jye, Yu, et al.** 1998, Mat Res Innov, pp. 2:181-188.

10. **Marek, Steve.** Chapter 25: Brazing. [book auth.] Hwaiyu Geng. *Manufacturing Engineering Handbook.* New York : McGraw-Hill, 2004, pp. 25.1-25.12.

11. **Gale, W. F. and Totemeier, T. C.** 33 Welding. *Smithells Metals Reference Book.* Burlington : Elsevier Butterworth-Heinemann, 2004.

12. **Sittig, Marshall.** *Cryogenics: Research and Applications.* Princeston : D. Van Nostrand Company, Inc., 1963.

13. **Cassiano, Cosimo.** *Anti-Noise Platen of the Flat Type for an Impact Printer. US 6,588,955* United States of America, July 8, 2003.

14. **Hitoshi, Kounan and Katsuhiko, Yokoi.** *Noise Reducing Back Stopper for an Impact Print Head. 5,149,213* United States, April 29, 1991.

15. **Ashby, Michael.** *Materials Selection in Mechanical Design.* Italy : Elsevier, 2005. ISBN-13: 987-0-7506-6168-3.

16. **Howard, Quincy and Enzukewich, Steve.** The Effects of Microstructure on Ultrazonic Testing of Alloy Steels. *The American Society for Nondestructive Testing.* [Online] The Boeing Company, 1997. [Cited: April 12, 2010.] http://www.asnt.org/publications/materialseval/solution/dec97solution/dec97sol.htm.